Journal of Computer-Aided Molecular Design, **16:** 683–709, 2002.
KLUWER/ESCOM

Structure-based QSAR study on differential inhibition of human prostaglandin endoperoxide H synthase-2 (COX-2) by nonsteroidal anti-inflammatory drugs

R. Pouplana[a*], J.J. Lozano[b], C. Pérez[a] & J. Ruiz[a]
[a]*Departament de Fisicoquímica, Facultat de Farmàcia, Universitat de Barcelona, Av. Joan XXIII, s/n, 08028 Barcelona, Spain;* [b]*Department of Physiology and Biophysics, Mount Sinai School of Medicine, NY, USA*

Received 1 May 2002; accepted in final form 11 November 2002

Key words: cyclooxygenase inhibitors, h-PGHS-2, COX-2, anti-inflammatory agents, NSAIDs, docking, COMBINE analysis, linear response method, molecular modelling, molecular dynamics, QSAR modelling.

Summary

The prostaglandin-endoperoxide H synthase-1 (PGHS-1) and prostaglandin-endoperoxide H synthase-2 (PGHS-2) are the targets of nonsteroidal anti-inflammatory drugs (NSAIDs)**.** It appears that the high degree of selectivity for inhibition of PGHS-2 shown by certain compounds is the result of two mechanisms (time-dependent, time-independent inhibition), by which they interact with each isoform. Molecular models of the complexes formed by indomethacin, sulindac, fenamates, 2-phenylpropionic acids and selective cyclooxygenase-2 (COX-2) inhibitors with the cyclooxygenase active site of human PGHS-2 have been built, paying particular attention to water molecules that participate in the hydrogen-bonding network at the polar active site entrance. The stability of the complexes has been assessed by molecular dynamics simulations and interaction energy decomposition analysis, and their biological significance has been discussed in light of available X-ray crystallographic and kinetic results. The selective PGHS-2 inhibitors exploit the extra space of a side-pocket in the active site of PGHS-2 that is not found in PGHS-1. The results suggest that active site hydration together with residues Tyr^{355}, Glu^{524}, Arg^{120} and Arg^{513} are crucial to understand the time-dependent inhibition mechanism. A marked relationship between the isoform selectivity and tightly interactions with residues into the side pocket bordered by Val^{523} is also found.

Introduction

Prostaglandins act as potent mediators of pain, fever and inflammation. The prostaglandin H synthase (PGHS) catalyses the conversion of arachidonic acid to the prostaglandin endoperoxide PGG_2 then PGH_2, which serves as the precursor for the formation of PGs and thromboxanes [1–4]. Two isoforms of PGHS have been identified [5]. The first, PGHS-1, is constitutively expressed in most tissues and is believed to generate prostaglandins for normal physiological functions. The second isoform, PGHS-2, is characterised by a rapid induction by a variety of stimuli, including mitogens, hormones, cytokines, and growth factors. The nonsteroidal anti-inflammatory drugs (NSAIDs) [6,7] exert their anti-inflammatory, antipyretic and analgesic effects by blocking the production of prostanoids from arachidonic acid through inhibition of PGHS activity. Recent human epidemiological studies suggest an inverse relationship between intake of NSAIDs and the risk of colorectal cancer [8,9], and the severity or incidence of Alzheimer's disease [5].

There are at least four categories of NSAID-mediated inhibition of PGHS-2; a) competitive, time-independent (ibuprofen, flufenamate and mefenamate); b) tight binding, time-dependent (indomethacin, flurbiprofen, ketoprofen, meclofenamate, diclofenac, NS-398, SC-558, SC-57666, celecoxib and SC-58125); c) weak binding, mixed (niflumate, naproxen and sulindac); and d) irreversible inhibitors

*To whom correspondence should be addressed.
E-mail: ramon@farmacia.far.ub.es

of PGHS-2 (aspirin and APHS). The mixed inhibition is characterised by an initial time-dependent loss in enzyme activity, which asymptotically approaches a non-zero limit. Time-dependent inhibitors of PGHS isozymes are generally more potent inhibitors than time-independent, competitive inhibitors. It appears that the high degree of selectivity for inhibition of PGHS-2 shown by certain compounds is the result of two different mechanisms (time-dependent, time-independent inhibition), by which they interacts with each isoform.

Essentially all NSAIDs in therapeutic use exhibit nonselective inhibition of both isoforms, whereas recently described diarylheterocycle compounds (Figure 2), such as SC-58125, SC-57666, SC-558, celecoxib and NS-398, are potent and selective inhibitors of PGHS-2 [10]. Kinetic analysis demonstrated that isoform selectivity was attained via elimination of the time-dependent component of inhibition on PGHS-1, but time-dependent inhibitors of PGHS-2 [11]. The fenamic [12,13] and 2-phenylpropionic acids [14] can be classified as competitive inhibitors of substrate binding that cause time-dependent or time-independent loss of cyclooxygenase activity to both PGHS isoforms. Meclofenamate, diclofenac, flurbiprofen, ketoprofen and indomethacin show a rapid time-dependent inhibitory effect for both isoforms. Flufenamate, mefenamate, niflumate, ibuprofen, naproxen and sulindac are partially time-independent inhibitors for both isoforms. Looking at structures (Figure 1), it seems that geometrical similarity is not a sufficient criterion to explain the time-dependent/time-independent inhibition of PGHS by these compounds, and that other properties should be included in the model for a more realistic description of the recognition process.

The X-ray crystal structures of ovine PGHS-1 and murine PGHS-2 reveal that the positioning of carboxylate-containing inhibitors (S-flurbiprofen, indomethacin) in the cyclooxygenase active site channel of the PGHS isoforms is such that the carboxylate group interacts with the guanidinium group of Arg^{120} of PGHS-1 [14] and the analogous Arg^{120} of PGHS-2 [16,17]. Other charged residues in the cyclooxygenase active site include Glu^{524} in PGHS-1, Glu^{524} and Arg^{513} in PGHS-2. The phenolic side chain of Tyr^{355} in PGHS-1 and PGHS-2 is present near the mouth of the channel opposite Arg^{120}. The biochemical, biophysical and molecular modelling studies [18,19,20] indicate that in PGHS-1, Arg^{120} is a key in the interaction with arachidonic acid and NSAIDs containing carboxylic acid groups. Inspection of the crystal structure of the ovine PGHS-1/S-flurbiprofen complex suggests that Arg^{120} forms a salt bridge with Glu^{524} and that Tyr^{355}, which is in close proximity to Arg^{120}, might determine the stereochemical specificity of PGHS-1 toward 2-phenylpropionic acid inhibitors [15]. However, the structure of PGHS-2 shows (Figure 3)) at least two possible hydrogen bonding arrangements near the entrance to the binding pocket: one consisting of Arg^{120}, Glu^{524}, and Tyr^{355} and another consisting of Arg^{513}, Glu^{510} and Tyr^{355}. It is possible that the disruption of the equilibrium between these two arrangements contributes to the slow binding for the time-dependent inhibition [21]. Finally, well ordered water molecules can be identified in the cyclooxygenase channels of the X-ray crystal structures of ovine PGHS-1 complexed to flurbiprofen (1EQH) and ibuprofen (1EQG) determined at similar resolution (2.7 and 2.61 Å) One molecule bridges the Tyr^{355} and the His^{90}. This water is hydrogen bonded to a second water, which in turn contacts Glu^{524}. An additional water molecule is hydrogen bonded to Ser^{530} and Tyr^{385} [22]. These waters are seen in all structures, and appear to play key roles in maintaining the structural integrity of the channel. Molecular modelling studies performed on the two isozymes suggest that active site hydration is also crucial for the selectivity of ketoprofen analogues [23].

The fact that most, but not all, nonselective NSAIDs contain a free carboxylic acid group (Figure 1) while all selective PGHS-2 inhibitors reported to date do not contain a carboxylic acid moiety raises the question about the role of the analogous Arg^{120} in PGHS-2, in mediating the binding of selective and nonselective PGHS inhibitors. Diclofenac and fenamates series of NSAIDs bind PGHS-2 so that the carboxylate group is not close to Arg^{120} [24]. All highly selective PGHS-2 inhibitors having a sulfonyl group interact with Arg^{120} or Arg^{513} in a manner similar to the interaction of the carboxylic acid group of flurbiprofen with Arg^{120} in PGHS-1 (Figure 2). However, there is ambiguity about the orientation of the sulphonamide in the two X-ray structures of SC-558 bound to COX-2 (1cx2 and 6cox) solved from crystals formed by the group at Searle [25].

Comparison of the crystal structures of PGHS-1 and PGHS-2 provides no definitive explanation for the differing behaviour of Arg^{120} between the two isozymes. Although the relatively hydrophobic environment around Arg^{120} is preserved in the two isozymes, Arg^{120} is involved in an extended electrostatic/hydrogen bond network with Glu^{524} and Arg^{513}

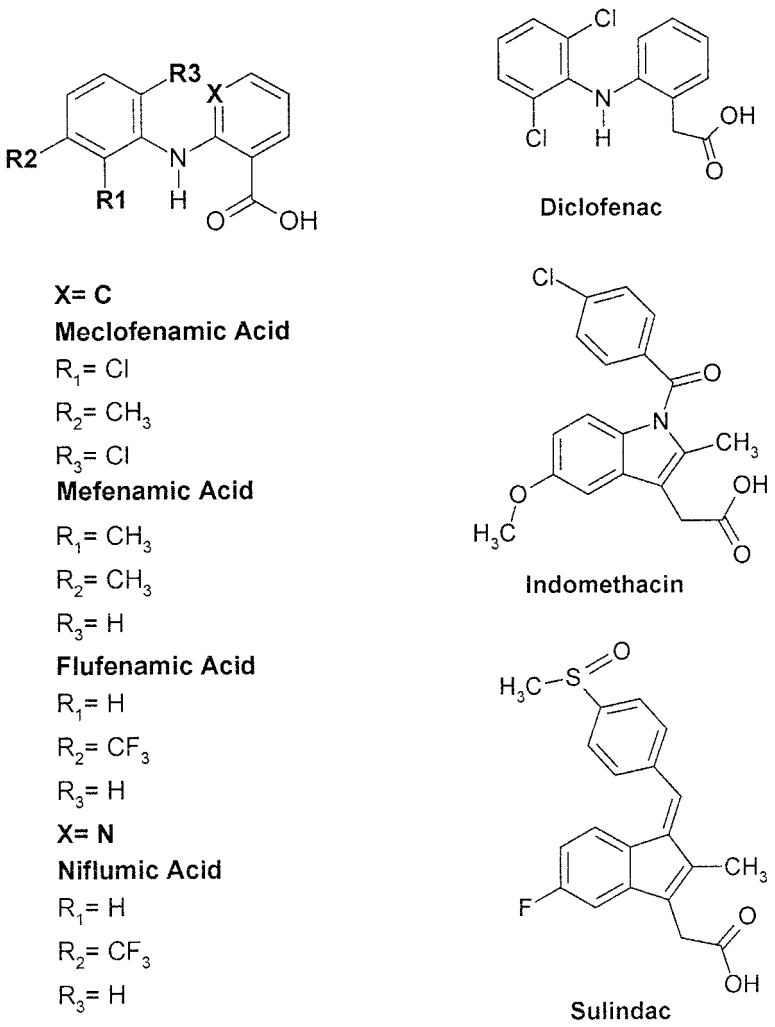

Figure 1. Structures of several fenamic, diclofenac, indomethacin and sulindac acids.

in PGHS-2. The differing hydrophobic and electrostatic environment could explain the observed differences in inhibitors binding between the two isoforms.

In the present work we have investigated the role of water molecules near the active site entrance of the PGHS-2 in mediating the binding of inhibitors and to rationalise the inhibition data. Molecular dynamics (MD) simulations in combination with a linear response [40,41] approach were used to estimate the free energies of binding for a series of 16 NSAID inhibitors of hPGHS-2. As shown here, combination of a docking protocol with a procedure for the accurate estimation of relative binding free energies can be valuable to clarify the origin of the COX-2/COX-1 selectivity. A comparative binding energy (Combine) analysis [42,43] also allows us to identify the most important enzyme-ligand interactions that account for the differences in activity within the series. Finally, analysis of molecular interaction fields [60], including the steric, electrostatic and lipophilic fields, is used to elucidate the different characteristics of the ligands in the COX-2/COX-1 selectivity. All this information can provide insight, which may conbe valuable to the development of NSAIDs with enhanced therapeutic potential and lower toxicity.

Methodology

Molecular modelling of NSAIDs

Molecular modelling of inhibitors was carried out on an O2 Silicon Graphics computer using the

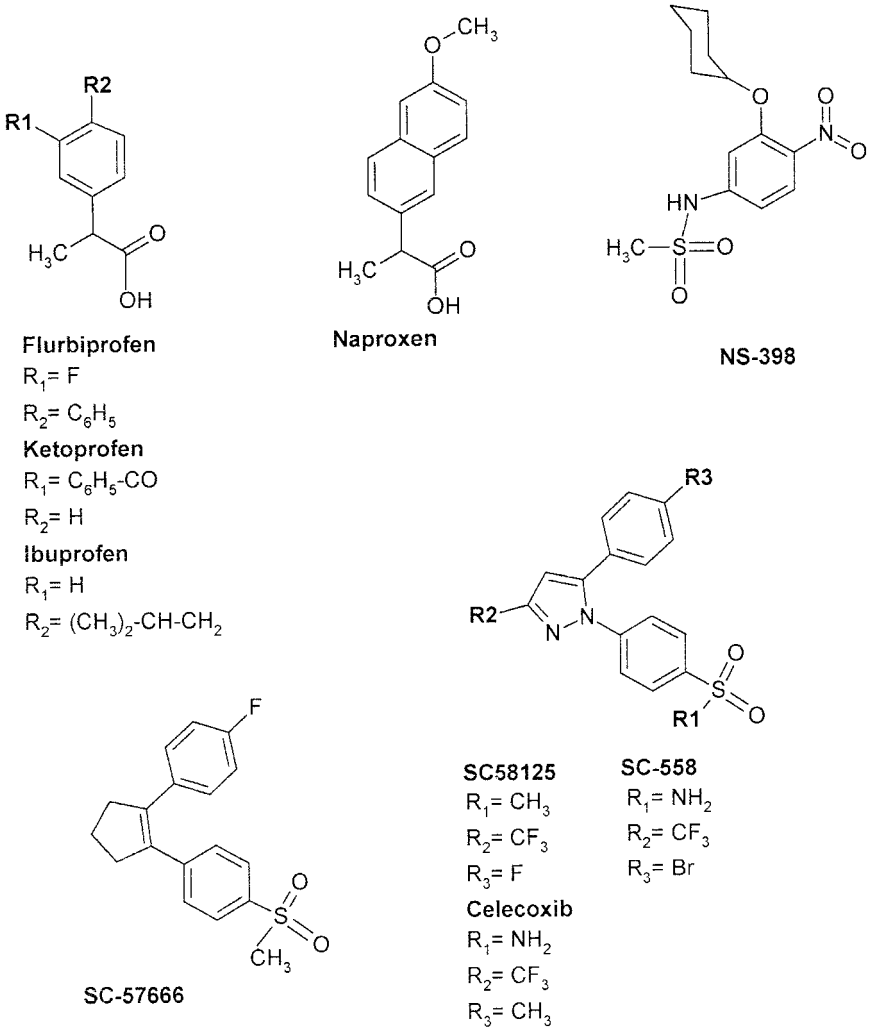

Figure 2. Structures of several 2-phenylpropionic acids and selective human COX-2 inhibitors.

Biosym/MSI molecular modelling software [28]. Molecular geometry (Figure 1) of indomethacin, diclofenac, meclofenamate, mefenamate, flufenamate, niflumate, flurbiprofen, ketoprofen, ibuprofen, sulindac and naproxen acids were obtained by combining X-ray crystallography data in the Cambridge Structural Database and conformational analysis [29–32]. For other compounds, SC-58125, celecoxib, SC-558, SC-57666 and NS-398 (Figure 2), conformational analysis was performed combining quenched molecular dynamics and energy minimisation techniques using the AMBER program [34]. The X-ray conformation was heated from 6 K to 600 K in 15 ps using classical molecular dynamics and a time step of 0.5 fs. After a further 25 ps of equilibration, it was slowly cooled down back to the initial temperature and energy minimized by using the conjugate gradient method until the root-mean-square gradient was less than 0.01 kcal mol^{-1} A^{-1}. The resulting structures were subjected to the same simulated annealing protocol, and the whole procedure was repeated 50 times. All conformers of the inhibitors having a rmsd greater 0.25 A and energies within 3 kcal/mol of the global minimum were used as the starting co-ordinate file in the docking study. The inhibitors were considered in the standard ionisation state at neutral pH, and their geometry was fully optimised at the ab initio HF/6-31G(d) level using the program Gaussian 96 [33]. Overall, there are four major conformational families that differ in the relative orientation of the aromatic rings and several subfamilies that arise from rotation about the R_1SO_2 bond. The energy differences among

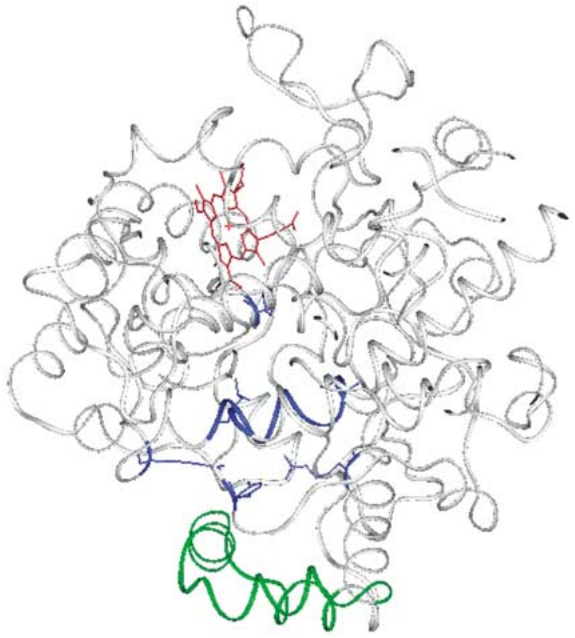

Figure 3. Ribbon representation of the modelled human COX-2 homomonomer. The heme prostetic group (red), the binding NSAIDs site with highlighted residues (blue) and hydrophobic side-chains (green) of the membrane binding domain are shown.

them were sufficiently small as to consider them all as candidates for the bound conformation.

NSAID docking in human PGHS-2 model

A model of human PGHS-2 (Figure 3), recently built in our group was used to examine the binding of inhibitors [27]. The AutoDock 3.0 program [35,36] was used to explore the docking for different conformations of the 16 NSAIDs in the active site of the enzyme. The AutoDock exploration was carried out within a 30-Å cube by using 0.25 Å grid spacing. Seven affinity grids were calculated (C,N,O,S,H,Cl,F). The simulated annealing protocol consisted of 100 runs of 50 cycles; each cycle including 25000 accepted or 25000 rejected relative positions. A distance dependent dielectric constant equal to 4r was used to simulate a partially solvated state. The annealing temperature was set to 310 K during the first cycle and then linearly reduced at the end of each cycle. Ligands were considered conformationally flexible by defining the torsion angles about which rotation was allowed. AutoDock was used to generate conformers within the binding site by randomly changing torsion angles and overall orientation of each molecule. From the 100 simulations with each compound, the binding mode with the lowest docked energy structures in the top ranked cluster was selected. To take into account protein flexibility, the stability and behaviour of all complexes was studied in a dynamic context and the van der Waals and electrostatic components of the interaction energy monitored. Further analysis of the binding orientation of the sulphonamide indicated that this substituent adopts the conformation presented in the crystal structure of 6cox [59].

The resulting ligand-enzyme complexes were analysed with the program GRID [37,38] for the presence of putative water molecule binding sites. A valuable starting point for this work was the presence of water molecules in the structure of the COX-1/flurbiprofen complex [22], which were successfully localised using GRID. Calculations were carried out in a standard lattice corresponding to a 4-Å extension of the ligand-plus-water ensemble ($31\times27\times26$ Å) with 1.0 Å grid spacing. In the next step, the program MINIM, included in the GRID package, was used to find favourable minima inside the same grid box (39). As expected, using a cutoff of -7 kcal/mol, the calculations showed several minima for each of the complexes but clearly all presented a unique minima within 2.0 Å of the position of the crystallographic waters in the cyclooxygenase channel. For each complex, four water molecules located by the GRID analysis were explicitly considered in subsequent studies.

Molecular dynamics simulations

The resulting complexes were energy minimised by molecular mechanics (MM) method in AMBER using a cutoff of 12.0 Å. Restricted electrostatic potential fitted charges determined at the HF/6-31G(d) level, and van der Waals parameters taken for related atom types in the AMBER-95 force field were used for each inhibitor. SHAKE was used to maintain all the bonds at their equilibrium distances and a nonbonded 12 Å cutoff and a distance-dependent dielectric constant were used throughout. In each case, 100 steps of steepest descent were followed by conjugate gradient until the root-mean-square value of the potential energy gradient was below 0.01 kcal mol^{-1} A^{-1}.

Ligand, GRID-positioned water molecules and a cap of 220 TIP3P water molecules centred at the inhibitor, together with the amino acids within 12 Å from the ligand, were used as input for the subsequent molecular dynamics simulation. The number of fragments was kept to a minimum by including some additional conecting residues including N-terminal,

methylacetamide and C-terminal capping residues on non-contiguous pieces of the protein. The lysine residues on the periphery of the system were neutralised to bring the total charge of the system to zero. The resulting systems were subjected to full conjugate gradient minimisation until the rms value of the potential energy gradient was below 0.01 kcal mol^{-1} A^{-1}, using the AMBER force field for all parameters except for the charges for the ligand atoms, which were obtained quantum mechanically as described above. First, for each mutated residue a short optimisation run restraining the backbone to their initial co-ordinates was conducted. This allowed readjustment of covalent bonds and van der Waals contacts without changing the overall conformation of the protein. Then, only the ligand atoms were allowed to move and finally the whole complex was energy minimised although the protein backbone atoms were restrained to their initial positions by a harmonic potential with a force constant of 32 kcal mol^{-1} A^{-1}, while the hydrogen atoms, the inhibitor and water molecules were unrestrained.

The resulting complexes were heated for 30 ps, equilibrated for 110 ps at 298 K and then 320 ps molecular dynamics was performed, under the same restraining conditions. Integration was carried out with time-step of 2 fs, with scaling factor 2.0 for 1–4 interaction. The non-bonded pair-list was upgraded after every 20 cycles and co-ordinates were saved every 10 ps from the last 200 ps and energy-minimised for further analysis of complexes. Calculations were performed using the AMBER computer program. The reported flexible nature of the hPGHS-2 binding site was taken into account in our molecular dynamics simulations, which were carried out for the two orientations of NS-398, celecoxib, SC-558 and SC-58125 suggested by the automated docking program.

Linear response (LR) method

The LR method [40,41] relies upon free energies calculated from averages based on termally equilibrated collections of configurations. For each inhibitor two MD simulations were performed, one for the unbound inhibitor in solvent and a second with the inhibitor bound in a 102-residue PGHS-2 binding site pocket in solvent models, using the crystallographic water molecules and a cap of 220 TIP3P water molecules centred at the inhibitor. The starting conformation for the unbound inhibitors and for the inhibitor-enzyme complex was obtained from the refined complexes. The MD simulations consisted of an initial solvent equilibration for 30 ps equilibrated for 110 ps at 298 K and then a 500 ps molecular dynamics was performed. Integration was carried out with time-step of 2 fs, with scaling factor 2.0 for 1–4 interaction. Energy averages were then accumulated over final 500 configurations during which atomic co-ordinates were saved after each 1ps. Separate running averages were determined for the Lennard-Jones and coulombic components of the nonbonded interaction energies. Calculations were performed using the AMBER5 computer program. In the LR framework, the binding affinity can be expressed as noted in Equation 1, where the U^{vdw} and U^{elec} refer to the Lennard-Jones and electrostatic average interaction energies for the bound and unbound states of the inhibitor, and the third term is included to account for the cost of creating a cavity in the solvent. The coefficients α, β and δ are empirically determined to obtain the best fit to the experimental data.

$$\Delta G_{binding} = \alpha((U^{vdw}_{bound}) - (U^{vdw}_{unbound})) + \beta((U^{elec}_{bound}) - (U^{elec}_{unbound})) + \delta \quad (1)$$

Comparative binding energy (COMBINE) analysis

Ligand-enzyme interaction energies of the refined complexes were calculated and partitioned on a per residue basis using the ANAL module of the AMBER program. Each solvated ligand or residue was regarded as a single fragment and no intramolecular energy terms were considered. Since the 102 residues of COX-2 were independently considered in the partitioning scheme, and three energy contributions (van der Waals, electrostatic and hydrogen bonding) were calculated for each residue, 310 energy variables were used to characterise each complex. The resulting energy matrix was pre-treated by zeroing all the variables with absolute values lower than 0.05 kcal/mol and by removing those with a standard deviation below 0.05 kcal/mol. The variables were divided into two blocks: a van der Waals block and an electrostatic block. In order to equalise the importance of the blocks of variables the Block Unscaled Weight (BUW) method was used. Finally, three consecutive functional factorial design (FFD) variable selections were performed over the matrix obtained after pre-treatment. The optimal dimensionality of the PLS models was determined by monitoring the cross-validation indexes as a function of the number of latent variables extracted. For cross-validation, the compounds were assigned randomly to any of five groups of approximately the

same size, and the whole procedure was repeated 20 times. The predictive ability of the resulting models is reported by both the cross-validated correlation coefficient (q^2), and the standard deviation of error of predictions (SDEP). Calculations were performed using the COMBINE computer program (provided by A.R. Ortiz).

Alignment of the compounds

The NSAID conformation extracted from the MD refined inhibitor-enzyme complexes was used as template for molecular alignment, assuming that this conformation represents the most probable bioactive conformation of the 2-phenylpropionic, indolacetic, fenamic acids or diarylheterocycle derivatives at the enzyme active site level.

GRID force field

The program GRID (36, 37) was used to calculate the interactions between a small chemical group (probe) and each of the 16 ligands (target). The probes selected for this study include the methyl group (C3), phenolic group (OH), the sp^2 amine NH_2 cation (N2=), water and hydrophobic probes. All GRID calculations were performed using 0.5 Å spacing, between the grid points in a rectangular box measuring $30\times23\times26$ Å. The GRID origin and axes were chosen such that all the atoms of the ligand (in the bound conformation), and an additional region that includes active site residues and water molecules within 4 Å from the ligand (protein residues were not explicitly included in the calculations). A cut-off of +5 kcal/mol was used in order to make the data more symmetrically distributed about zero. The resulting grids were contoured at appropriate energy levels and graphically displayed to aid in the visualisation of complementarily regions with each of the selected conformers.

Molecular electrostatic potential maps and solvation

The free energies of solvation in aqueous solution were obtained from the resulting structures of the ligands in the refined complexes and fully optimised at the ab initio HF/6-31G(d) level by IPCM solvation model using the program Gaussian 96.

The electrostatic potential V generated at a point $\mathbf{r}_i$ for a molecular system with electron density function $\rho(\mathbf{r})$ is given by

$$V(r_i) = \sum_A \frac{Z_A}{(r_i - R_A)} - \int \frac{\rho(r)}{(r_i - r)} dr$$

where $\mathbf{Z}_A$ is the charge on nucleus A, located at $\mathbf{R}_A$.

The molecular wavefunction was computed at the HF/6-31G(d) level. The MEP minima values were found with the MEPMIN program [44]. MEP minima energies and locations were determined for each molecule. The isopotential surfaces were obtained using the interpolation technique of the InsightII program [28].

Results

NSAID docking in human PGHS-2 model

Our homology modelling of the human enzyme was tested [27] with docking calculations using the AutoDock 3.0 program, which randomly manipulates a ligand to determine the most favourable bound conformation and orientation in the enzyme or receptor. After having refined the structures of the docked ligands by energy minimisation with the AMBER force field and a dielectric constant of 4r, the predicted binding mode closely reproduced the experimental structural data available for the human PGHS-2-flurbiprofen and human PGHS2-indomethacin complexes [22, 25]. Moreover, in all cases the ligand bind in a conformation was energetically very close to the low-energy minima conformation, which indicates a small energetic destabilization upon binding.

Inspection of the complex of the PGHS-2 with S-flurbiprofen (Figure 4), which is located in the hydrophobic channel, reveals that the binding mode is similar to that in PGHS-1. The carboxylate group of the drug forms a salt bridge with Arg^{120} and a hydrogen bond withTyr^{355}. The distal phenyl ring forms close van der Waals contacts with Val^{523}, and the fluorophenyl ring also interacts with Val^{349} and Ala^{527} and stacks tightly against Tyr^{385}. In the case of indomethacin (Figure 4), the drug fills the entire hydrophobic channel from Tyr^{385} downward a distance of roughly 12–14 Å and forms a salt bridge with Arg^{120}. The chlorophenyl group lies in a hydrophobic pocket at the top the channel, the carbonyl group is situated at 3.4 Å from Ser^{530}, and the indole ring is in contact with several aliphatic side chains, including Val^{349}, Ala^{527}, Leu^{352}, Ser^{353} and Val^{523}. The *o*-methoxy group interacts closely with main-chain atoms of Tyr^{355} and Arg^{513}. Additional contacts are made with His^{89}, Met^{113}, Val^{116}, and Phe^{518}. It has been demonstrated [45–47] that these interactions produce significant effects on the binding affinity.

In the docked structures of flurbiprofen, ketoprofen, ibuprofen, naproxen (Figure 4), sulindac and

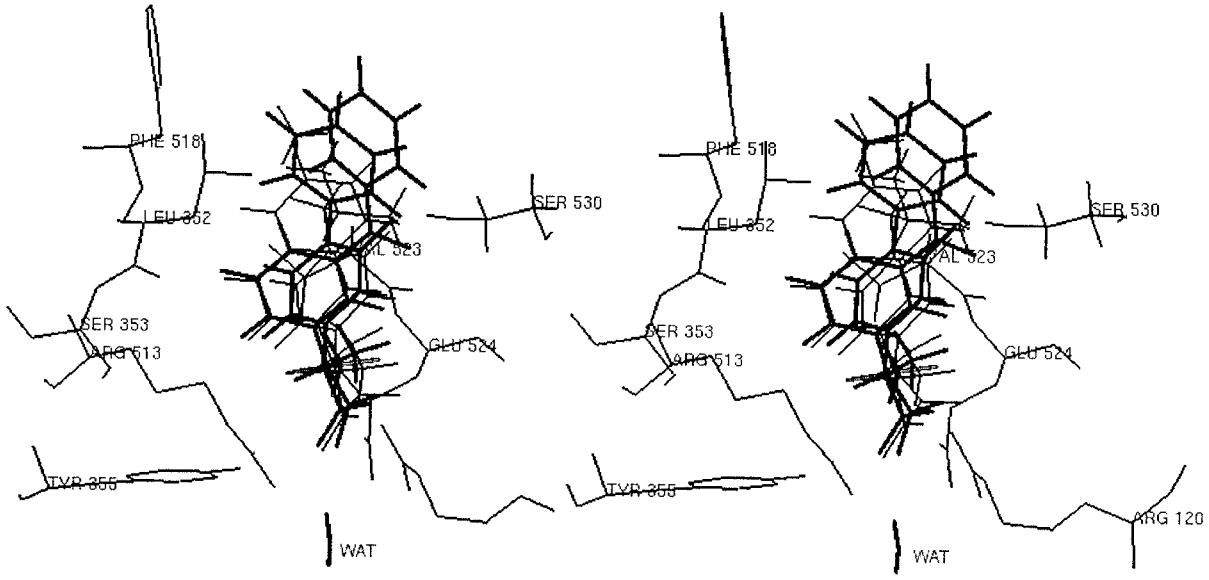

Figure 4. Model of S-flurbiprofen (black), S-ketoprofen (black), S-naproxen (grey) and S-ibuprofen (grey) in the cyclooxygenase-binding site (grey) of human PGHS-2 (in stereoview). Only water and residues relevant to the discussion are displayed.

indomethacin (Figure 5), a salt bridge between Arg^{120} and the carboxylate group of the drug is formed. This ionic interaction seems to be essential for the formation of a tight binding inhibitor complex leading to the time-dependent inhibition of PGHS by flurbiprofen, ketoprofen and indomethacin. Thus, as observed with ovinePGHS-1, the Arg^{120} group of hPGHS-2 is necessary for both efficient and time-dependent inhibition of hPGHS-2 by flurbiprofen [48].

The orientation of docked diclofenac, mefenamate, flufenamate, niflumate and meclofenamate (Figure 6) suggests that the contribution to the binding of an ionic interaction between the carboxylic acid group of these inhibitors with Arg^{120} of hPGHS-2 is poor. In the case of diclofenac, for instance, the carboxylic acid group of the drug appears to form a hydrogen bond with the hydroxyl of Tyr^{355}.

Weakly acidic inhibitors (Figure 7) possessing methylsulfoxide or sulphonamide group, NS-398, SC-558, SC-57666, celecoxib, and SC-58125, interact with Arg^{120} and Arg^{513} by two different binding orientations. The two binding modes are chemically reasonable, yielding similar interaction energies with the enzyme. In the orientation of NS-398 favoured by AutoDock, the nitrogen and oxygen atoms of the sulphonamide group interact with Arg^{120} and the nitro group is in the side pocket close to Arg^{513}. Moreover, the phenoxy ring occupies a position perpendicular to the aromatic ring of the Tyr^{385}. This binding mode would reproduce the experimental evidence available for this drug [46–49]. The interaction of the sulphonyl group of the SC-558, SC-57666, celecoxib and SC-58125 shows that the phenylsulfonamide or phenylmethylsulfoxide group is accommodated in the side pocket around Val^{523} of the PGHS-2 active site with the oxygen atoms of the sulphonyl group hydrogen-bonded to Arg^{513}. The docking results showed that SC-558, SC-57666, celecoxib and SC-58125 occupies a position comparable to that of the SC-558 in its complex with mouse COX-2 [24, 48].

As observed with ovine PGHS-1 [18], the Arg^{120} group of hPGHS-2 seems necessary for both efficient binding and time-dependent inhibition of hPGHS-2 by non PGHS-2-selectivity inhibitors. Furthermore, the guanidino group of Arg^{120} actually interferes with the binding of PGHS-2-selective inhibitor [49]. The selective inhibitors interact closely with main-chain atoms of Leu^{352}, Ser^{353} and Val^{523} in the zones surrounding the first aromatic ring. Thus, the single Val^{523} to Ile mutation of PGHS-2 results in a loss of sensitivity to inhibition by NS-398 and SC-58125, suggesting that these atoms enhance the time-dependent affinity for PGHS-2 [50].

Molecular dynamics simulations

The 16 docked receptor-ligand complexes were studied in a dynamic context to take into account pro-

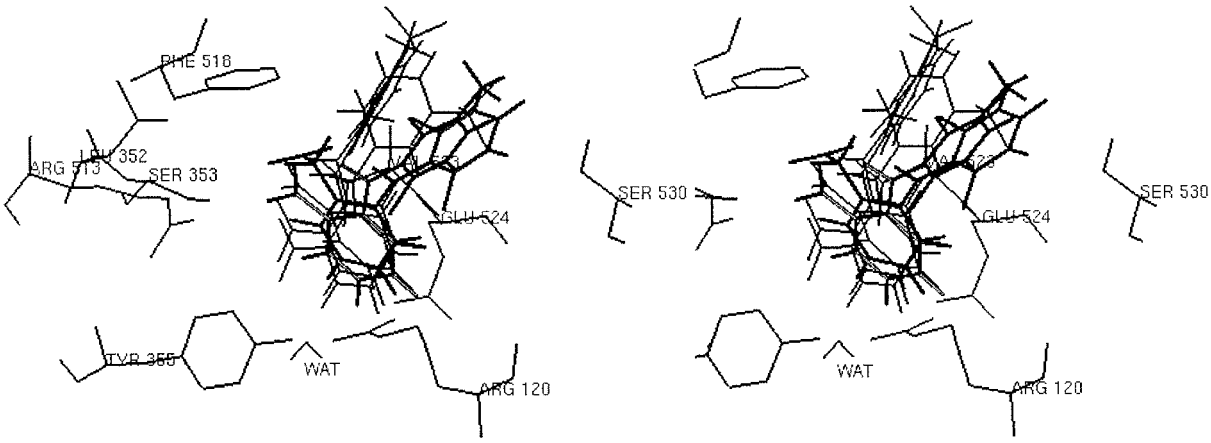

Figure 5. Model of meclofenamate (black), diclofenac (black), mefenamate (grey), flufenamate (grey) and niflumic (grey) in the cyclooxygenase-binding site (grey) of human PGHS-2 (in stereoview). Only water and residues relevant to the discussion are displayed.

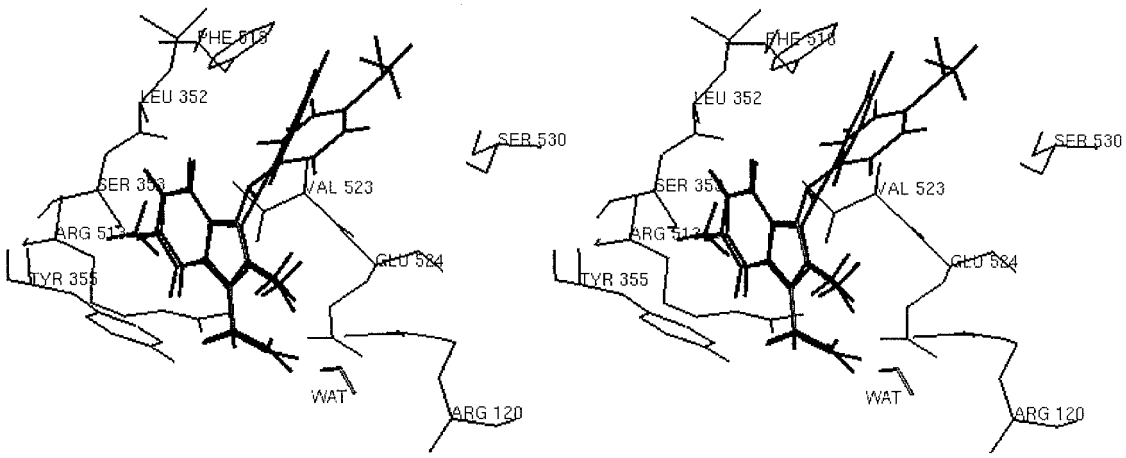

Figure 6. Model of *cis*-indomethacin and sulindac (black) in the cyclooxygenase binding site channel (grey) of human PGHS-2 (in stereoview). Only water and residues relevant to the discussion are displayed.

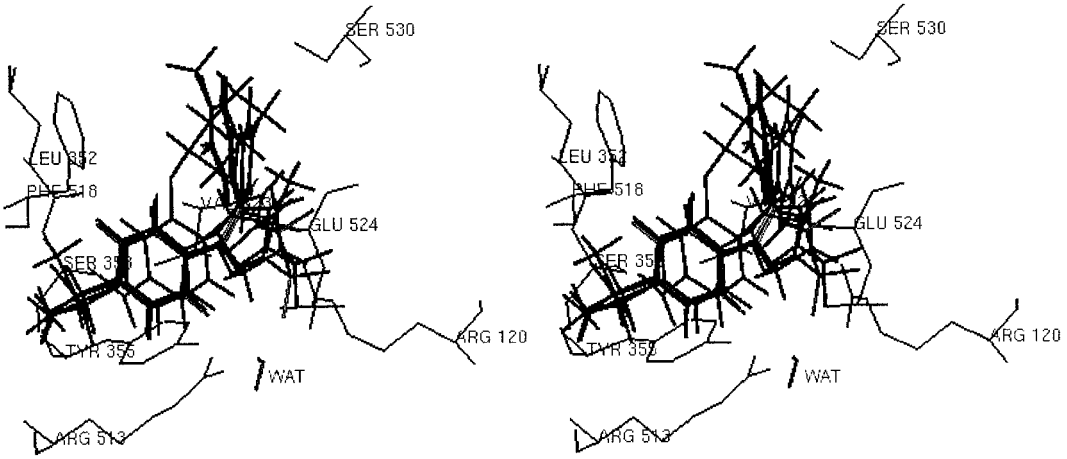

Figure 7. Model of SC-558 (black), SC-58125 (black), SC-57666 (black), celecoxib (black) and NS-398 (grey) in the cyclooxygenase-binding site channel (grey) of human PGHS-2 (in stereoview). Only water and residues relevant to the discussion are displayed.

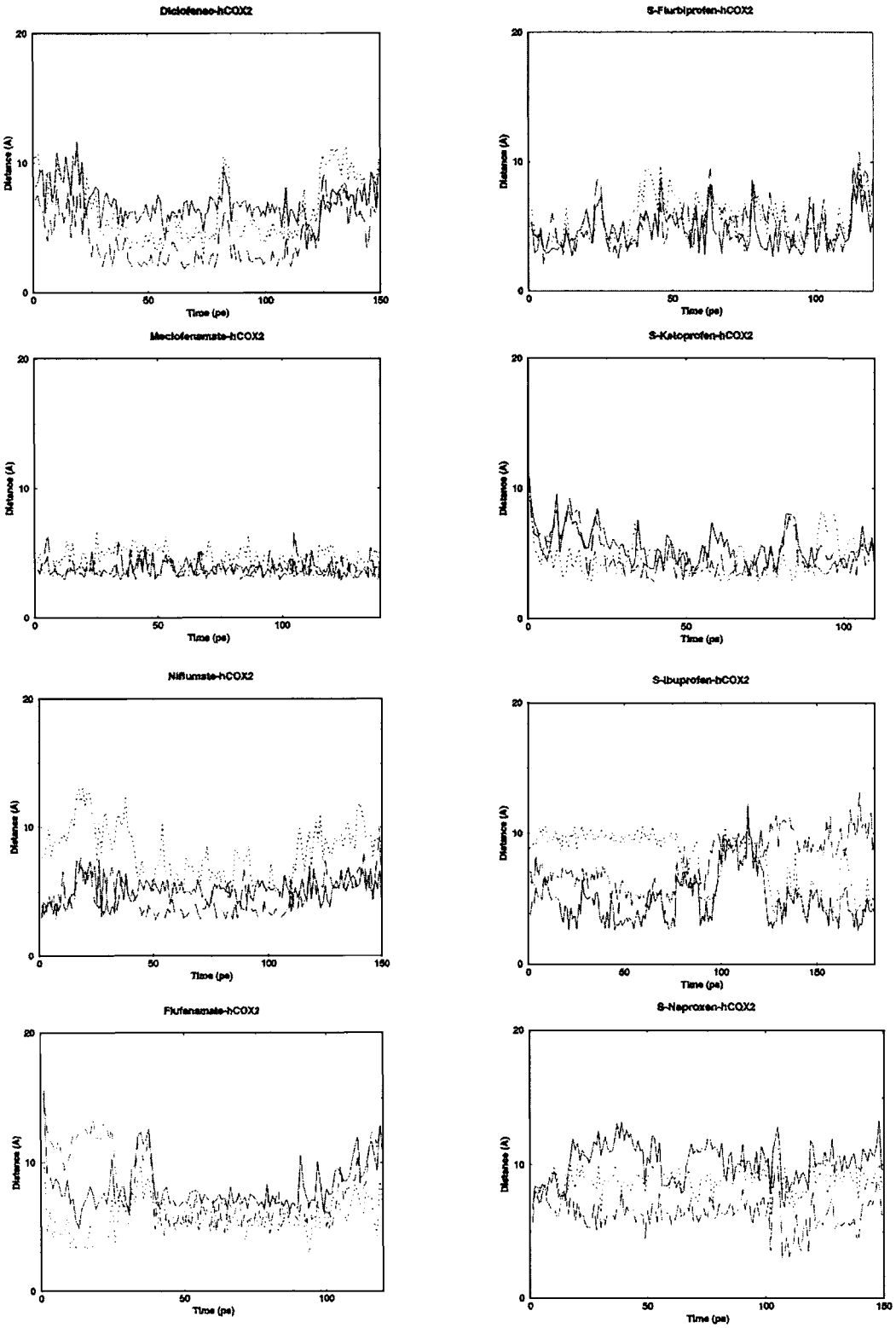

Figure 8. Monitored distance between the water molecule oxygen atom and the ligand carboxylate carbon atom (- - - -), the Arg^{120} guanidine carbon atom (– – –) and the Tyr^{355} phenol oxygen atom (. . .) in all inhibitor-h PGHS-2 complexes.

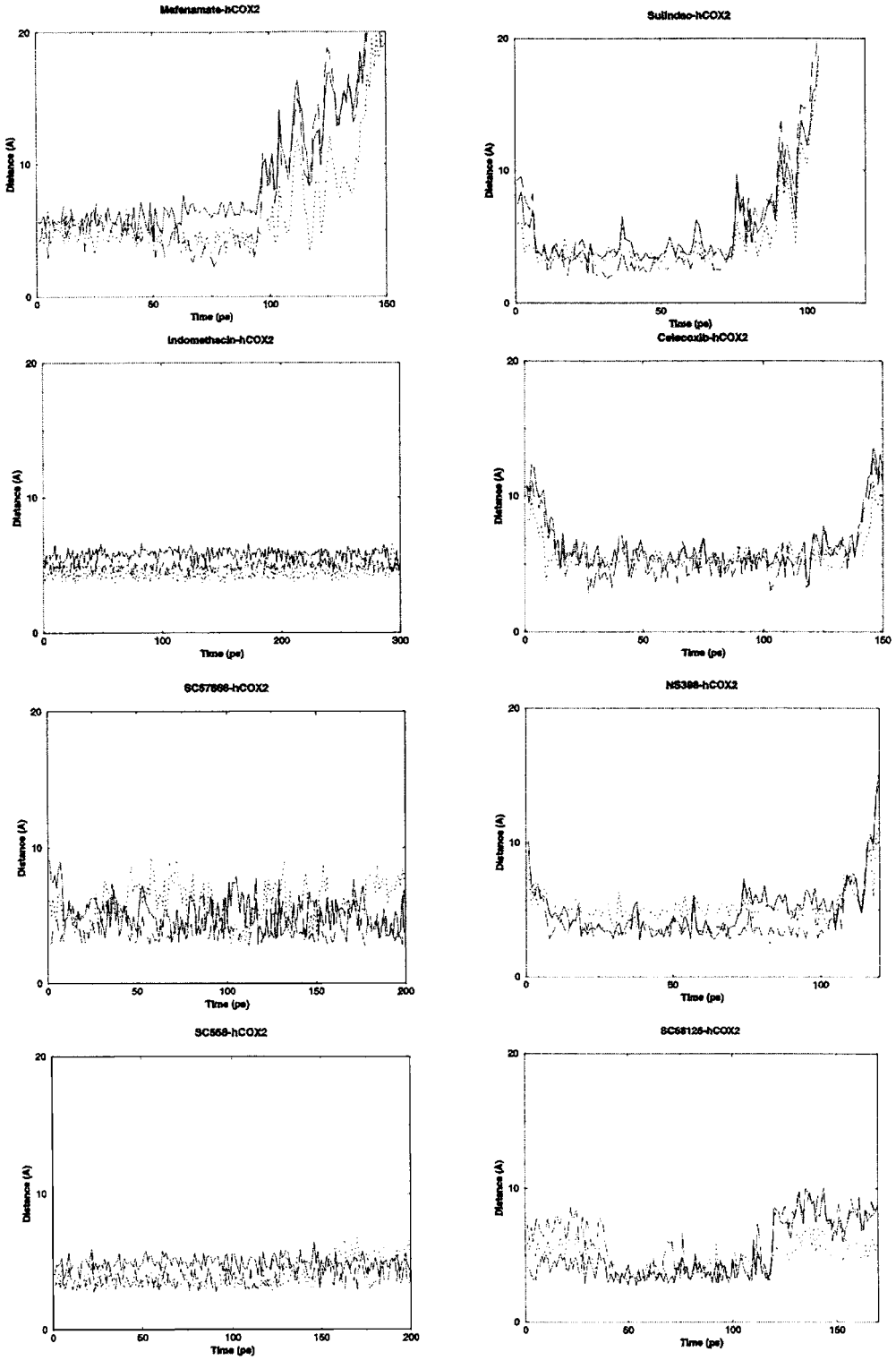

Figure 9. Monitored distance between the water molecule oxygen atom and the ligand carboxylate carbon atom or ligand R2 atom for selective COX-2 inhibitor (- - - -), the Arg^{120} guanidine carbon atom (– – –) and the Tyr^{355} phenol oxygen atom (. . .) in all inhibitor-h PGHS-2 complexes.

tein flexibility and the possibility of conformational changes and the van der Waals and electrostatic interaction energies between receptor and ligand were monitored along the molecular dynamics simulation. The structural analysis showed that the complex remains stable along all the simulations without suffering remarkable changes in the interactions with the enzyme residues contributing to the binding. The distances between the inhibitor and the water molecule and between the latter and the amino acids Arg^{120} and Tyr^{355} were monitored (Figures 8–9). This water molecule participates in the dynamic hydrogen-bonding network at the polar active site entrance. Particularly, it forms a hydrogen bond with the guanidine group of Arg^{120} and with the hydroxyl group of Tyr^{355}. The results indicate that a stable complex between inhibitor, water molecule and the residues Arg^{120} and Tyr^{355} is found only for the time-dependent arylacetic (flurbiprofen and ketoprofen), fenamate (diclofenac and meclofenamate), indomethacin and selective COX-2 (SC58125, SC57666, SC558, NS-398 and celecoxib) inhibitors, where the hydrogen-bonded network remains stable along the MD trajectory, even after a temporary migration. In contrast, in the case of mixed time-dependent inhibitors (naproxen, niflumate and sulindac) and time-independent inhibitors (flufenamate, ibuprofen and mefenamate) the water molecule moved away from the hydrogen-bonded network. The observed differences in the dynamic behaviour of the complexes together with the parallelism with the activities add support to the mechanism kinetics observed for the inhibition of COX-2 by NSAIDs.

The energy contributions to the binding of the inhibitor to residues in the active site obtained after energy-minimisation of the receptor-ligand complex are shown in Table 1. The differences in interaction energy arise mainly from electrostatic and van der Waals contributions emanating from the carboxylate and sulphonyl groups. It can be seen that the major contributors to the binding energy involve residues Arg^{120}, Leu^{352}, Ser^{353}, Tyr^{355}, Arg^{513}, Val^{523} and Ser^{530}. The selective inhibitors interact closely with main-chain atoms of Leu^{352}, Ser^{353} and Val^{523} in the zones surrounding the first aromatic ring.

In the AMBER-refined complexes for the NS-398 the overall intermolecular interaction energy is very similar in the two orientations, the van der Waals interaction being slightly more favourable in the orientation that places the sulphonamide group close to Arg^{120}. The other selective inhibitors place (Figure 7 and Table 1) the sulphonyl group close to Arg^{513} and His^{89} (one of the oxygen atoms contacts Arg^{513}, and the other oxygen is linked by hydrogen bond to His^{89}), giving rise to a more favourable electrostatic interaction in this orientation. The cyclooxygenase active site forks at the SC-58125, SC-558, SC-57666 and celecoxib in the binding site. Hydrophobic residues Leu^{352}, Phe^{518}, and Val^{523} surround the phenyl ring. The R3-phenyl ring of these inhibitors binds a hydrophobic cavity formed by Phe^{401}, Leu^{384}, Tyr^{385} and Trp^{387}. The trifluoromethyl group of these inhibitors is bound to an adjacent pocket formed by Met^{113}, Val^{116}, Val^{349}, Tyr^{355}, Leu^{359} and Leu^{531}. These two binding sites have rough equivalents in the binding of arylacetics and indomethacin. The distal ring of arylacetics overlaps with the fluorophenyl ring of SC-58125, the first ring superimposes on the pyrazole of SC-58125 and the carboxylate of arylacetics and the trifluoromethyl group of SC-58125 binds to the same cavity.

The most striking result is that both, meclofenamate and diclofenac (Figure 6), bind PGHS-2 so that the carboxylate group of these inhibitors is not in close proximity to Arg^{120} but show at least two possible hydrogen bonding schemes near the entrance to the cyclooxygenase binding pocket, involving contacts with either Arg^{120} or Tyr^{355}, respectively.

Linear response (LR) method

The experimental IC_{50} values at 25^oC for NSAIDs [10, 51] were converted into estimated binding free energies ($\Delta G_{exptl} = RT \ln (IC_{50})$), which are given in Table 1. Although not formally equivalent, relative activities should correspond to relative free energies of binding for closely related series of inhibitors. Within the framework of the linear response theory, Equation 2 shows the best two-descriptor equation obtained by fitting the experimental activities of the 16 compounds.

$$\Delta G_{calcd} = 0.315\Delta U^{vdw} - 0.559\Delta U^{elec} - 1.044 \quad (2)$$

The correlation coefficient r^2 of 0,69 reflects reasonable agreement between theory and experimental ($F = 17.30$). In these calculations the inhibitor derivatives of arylacetics, fenamics and indolacetics were considered in the standard ionisation state, at normal physiological conditions neutral. The ΔU^{vdw} values (Table 2) are attractive and similar in magnitude to those for the neutral inhibitors. More favourable inhibitor-protein

Table 1. Residue-based energy decomposition of the interaction energy (kcal/mol) between inhibitors and the cyclooxygenase active site of PGHS-2 in the orientations bound studied.

INHIBITOR	ΔG_{bind}	Energy	INH..R120	INH..L352	INH..S353	INH...Y355	INH.. R513	INH..V523	INH..S530	R120..E524	R513..E524
S-Flurbiprofen	−10.5	VdW	−0,6	−4,0	−2,1	−2,2	−0,3	−3,5	−0,4	−1,0	−1,7
		Elec	−10,1	−0,3	0,0	−3,1	−1,2	0,3	−0,2	−10,9	−6,2
S-Ketoprofen	−10.2	VdW	−0,7	−3,5	−1,7	−2,2	−0,1	−3,8	−0,7	−0,6	−2,8
		Elec	−9,7	0,1	−0,0	−0,1	−1,0	0,7	−0,4	−12,5	−4,1
S-Ibuprofen	−6.3	VdW	−2,0	−2,0	−0,9	−2,0	−0,1	−2,9	−1,7	0,8	−1,6
		Elec	−9,1	−0,1	−0,0	−2,1	−1,0	0,3	−0,3	−11,2	−3,2
S-Naproxen	−7.8	VdW	−0,4	−3,8	−1,1	−2,1	−0,2	−5,0	−0,6	0,8	−2,2
		Elec	−9,9	−0,2	0,1	0,3	−1,0	0,2	0,0	−11,4	−3,1
Diclofenac	−11.6	VdW	−0,8	−0,5	−1,7	−1,1	−0,0	−2,9	−1,8	1,1	−0,1
		Elec	−0,7	−0,3	−0,8	0,2	−0,5	0,0	−0,3	−9,0	−0,8
Meclofenamate	−11.7	VdW	−1,3	−0,2	−1,6	−1,6	−0,1	−3,1	−2,0	−1,2	−0,1
		Elec	−1,7	−0,3	−3,3	0,1	−1,4	−0,1	−0,2	−8,6	−0,9
Mefenamate	−9.3	VdW	−2,5	−2,1	−0,6	−0,4	−1,7	−3,6	−2,3	0,4	−0,2
		Elec	−3,4	−0,3	−0,1	0,2	−7,0	−0,0	−0,2	−12,3	−1,8
Flufenamate	−7.5	VdW	−1,6	−2,5	−0,7	−1,0	−0,5	−3,5	−1,7	−0,8	−0,2
		Elec	−3,7	−0,2	0,0	0,1	−9,7	−0,2	0,0	−11,8	−1,4
Niflumate	−7.9	VdW	−2,6	−0,2	−1,7	−1,4	−0,1	−4,5	−1,4	−3,8	−0,1
		Elec	−1,8	−0,2	−2,8	0,0	−1,2	0,0	−0,3	−5,8	−0,9
Indomethacine	−10.3	VdW	−2,6	−1,0	−2,5	−2,3	−1,3	−4,6	−1,5	−0,2	1,4
		Elec	−10,1	0,0	0,0	−0,3	−1,6	0,0	−0,1	−9,2	−8,3
Sulindac	−9.2	VdW	−0,8	−2,0	−2,1	−1,7	−2,5	−4,2	−2,3	−1,4	1,0
		Elec	−7,4	0,0	−0,0	−0,0	−3,1	0,1	−0,2	−11,4	−7,9
Celecoxib	−10.5	VdW	−5,0	−1,6	−4,8	−2,4	−2,2	−4,9	−2,0	0,0	0,7
		Elec	−0,0	−0,5	−0,0	−0,6	0,0	−0,1	−0,1	−10,6	−9,6
SC58125	−9.9	VdW	−1,4	−3,7	−4,4	−0,8	−1,9	−5,4	−1,8	−1,5	0,0
		Elec	0,0	−0,5	−0,5	−0,1	−1,4	−0,4	0,2	−7,0	−8,0
SC558	−11.3	VdW	−4,8	−1,4	−3,5	−3,0	−2,9	−5,5	−1,8	−0,1	−0,8
		Elec	−1,1	−0,4	−0,0	−0,5	−0,2	−0,1	−0,1	−9,1	−7,2
SC57666	−11.3	VdW	−2,9	−0,9	−3,6	−0,7	−1,9	−4,9	−2,3	−1,2	−0,3
		Elec	0,4	−0,4	0,1	0,0	−0,3	−0,2	−0,1	−10,0	−8,4
NS398	−9.9	VdW	−2,3	−1,9	−2,9	−2,4	−2,0	−4,0	0,9	−0,4	0,3
		Elec	−2,8	0,0	0,0	−0,3	−1,3	−0,2	−0,2	−11,2	−8,0

van der-Waals interactions indicate a good steric fit and enhance binding. The van der Waals terms are all highly attractive and the value of this term correlates in a reasonable fashion with inhibitory activity ($r = 0.43$).

As might be expected from the favourable solvation of a charged species (see below), the ΔU^{elec} values are generally positive. This is reflected in the free energies of solvation in aqueous solution of the ligands, which are reported in Table 2. The hydration free energies range between −90 and −55 kcal/mol and between −18 and −13 kcal/mol for charged and neutral ligands, respectively. Among the charged inhibitors, flurbiprofen, ketoprofen, naproxen, diclofenac, meclofenamate, indomethacin and sulindac present the lowest free energies of solvation. In general, the more active NSAIDs acids show the lowest $\Delta G_{solvation}$ in aqueous solution. In fact, it has been estimated that the loss of hydrogen bonds upon binding of the ligand relative to the free hydrated state costs around 2 kcal/mol to the free energy of binding [40].

There still remains, however, a general trend that more active inhibitors have larger ΔU^{vdw} values (Table 2). The activities calculated by the LR equation (Figure 10B) were, in general, quite similar to the ex-

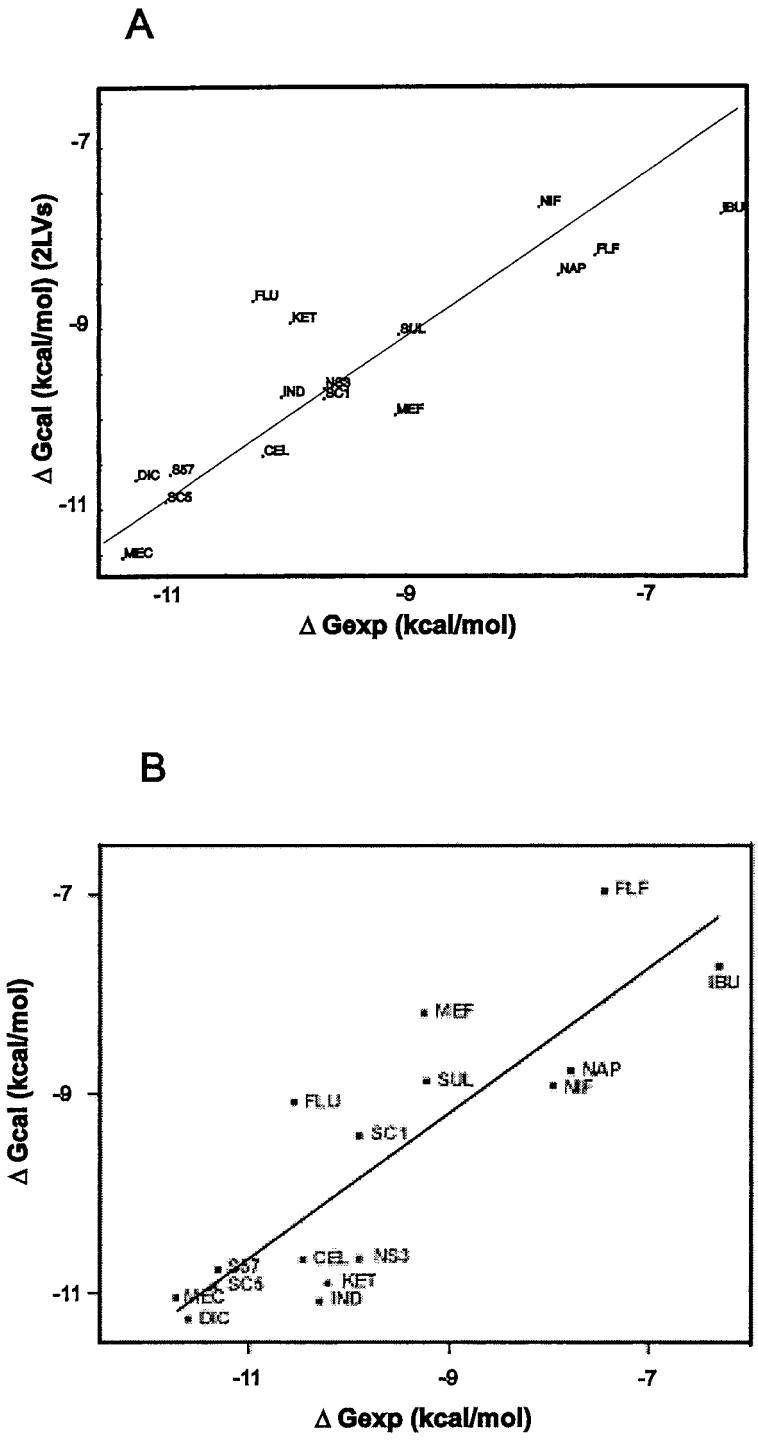

Figure 10. (A). Scatter plot showing the calculated versus experimental activity values of the COMBINE model. (B). Calculated binding affinities (ΔG_{cal}) using the Linear Response model versus experimental activities (ΔG_{exp}) for 16 inhibitors of COX-2.

Table 2. Changes in energy from MD simulations using bond and unbound inhibitors and free energy of solvation from QM calculations using unbound inhibitors.

Compound	ΔU_{vdw} (kcal/mol)	ΔU_{elec} (kcal/mol)	ΔG_{solv} (kcal/mol)
S-Flurbiprofen	−17.5	4.5	−89.1
S-Ketoprofen	−19.9	6.4	−71.3
S-Naproxen	−18.7	3.3	−73.3
S-Ibuprofen	−16.7	2.5	−70.0
Diclofenac	−19.6	7.2	−69.8
Meclofenamate	−20.3	6.5	−69.0
Mefenamate	−17.7	2.8	−67.4
Flufenamate	−18.3	0.3	−68.3
Niflumate	−18.6	3.6	−55.1
Indomethacin	−27.0	2.7	−69.0
Sulindac	−29.8	−2.8	−83.5
Celecoxib	−31.5	−0.6	−14.8
SC-58125	−24.4	1.2	−17.4
SC-558	−29.8	0.9	−16.2
SC-57666	−24.3	3.7	−13.2
NS-398	−26.1	2.5	−17.1

perimental values, with the exception of flurbiprofen, mefenamate, flufenamate and ibuprofen.

COMBINE analysis

In order to assess the optimal number of latent variables (LV) to include in the PLS [58] model, indexes of the fitting (r^2) and predictive (q^2) power of the models were plotted against the model dimensionality. The maximum quality was obtained for a model with 3 LV, but the slight improvement in comparison to a model with two LV and the small sample size ($n = 16$) recommend the use of the model with only 2 LV. This model includes 68 original variables in the PLS model and exhibits $r^2 = 0.77$, $q^2 = 0.64$ and SDEP (standard deviation of error of predictions) = 0.47. The activities calculated by the COMBINE model (Figure 10A) were, in general, quite similar to the experimental values, with the exception of flurbiprofen, ketoprofen, mefenamate, niflumate, flufenamate, naproxen and ibuprofen. It is worth noting that the determination of IC_{50} values depend on several factors, such as the source of enzyme activity, where there is species variability, use of recombinant enzymes or cell versus purified enzymes, pre-incubation times or measurement methods, which make difficult a direct comparison of data taken from different sources. As an example, published selectivity ratios for one of the earliest PGHS-2 selective inhibitors, NS-398, have ranged from 11 to > 1000-fold [43–45].

In a COMBINE model, the values of the weighted PLS pseudo-coefficients can be analysed to identify the most relevant ligand-residue interactions. The signs of those coefficients correlate with an increase (negative) or a decrease (positive) in activity. The most important residues in terms of steric or electrostatic interactions are shown in Table 1. Four areas in the binding site were described in the COMBINE analysis. An important region is located near the entrance to the cyclooxygenase-binding pocket; it can be interpreted as reflecting the possibility of the ligand to make water-bridged hydrogen bonds with Arg^{120} and Tyr^{355}. Remarkably, the negative PLS coefficients for Arg^{120} and Tyr^{355} correspond to the water-bridged interactions observed for the most active compounds between polar groups in the ligands and those residues. The second region is adjacent to the dynamic hydrogen-bonding network at the polar active site entrance. The more active compounds place their first ring in a region of the active site (Ser^{353}) that is unoccupied in four of the five complexes formed by the less active compounds (ibuprofen, naproxen, flufenamate and mefenamate). The only exception is niflumate, which adopts the orientation of the most active compounds, though it is a low-activity compound. Different residues of third region make favourable contacts with the first ring (Ser^{530} and Val^{523}), and

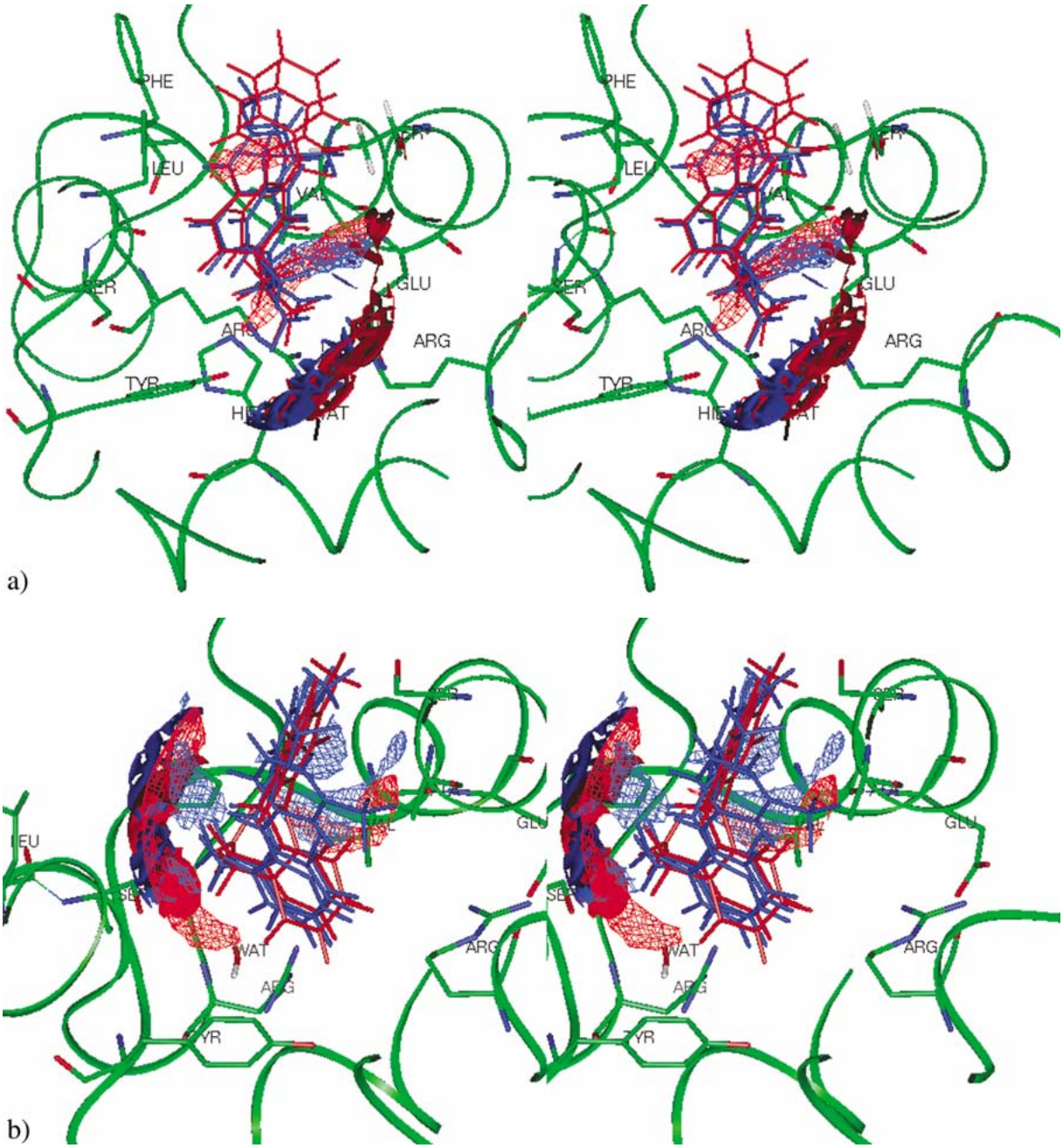

Figure 11. Model of the inhibitors in the cyclooxygenase-binding site (green) of human PGHS-2 (in stereoview). Only residues relevant to the discussion are displayed. The isopotential surfaces at −6.5 kcal/mol using phenolic hydroxyl probe and −1.75 kcal/mol using methyl probe determined from GRID calculations are shown. Calculations were carried out for: a) S-flurbiprofen (red), S-ketoprofen (red), S-naproxen (blue) and S-ibuprofen (blue); b) meclofenamate (red), diclofenac (red), mefenamate (blue), flufenamate (blue) and niflumic (blue); c) *cis*-indomethacin (red) and sulindac (blue); d) SC-558 (red), SC-58125 (red), SC-57666 (red), celecoxib (red) and NS-398 (blue).

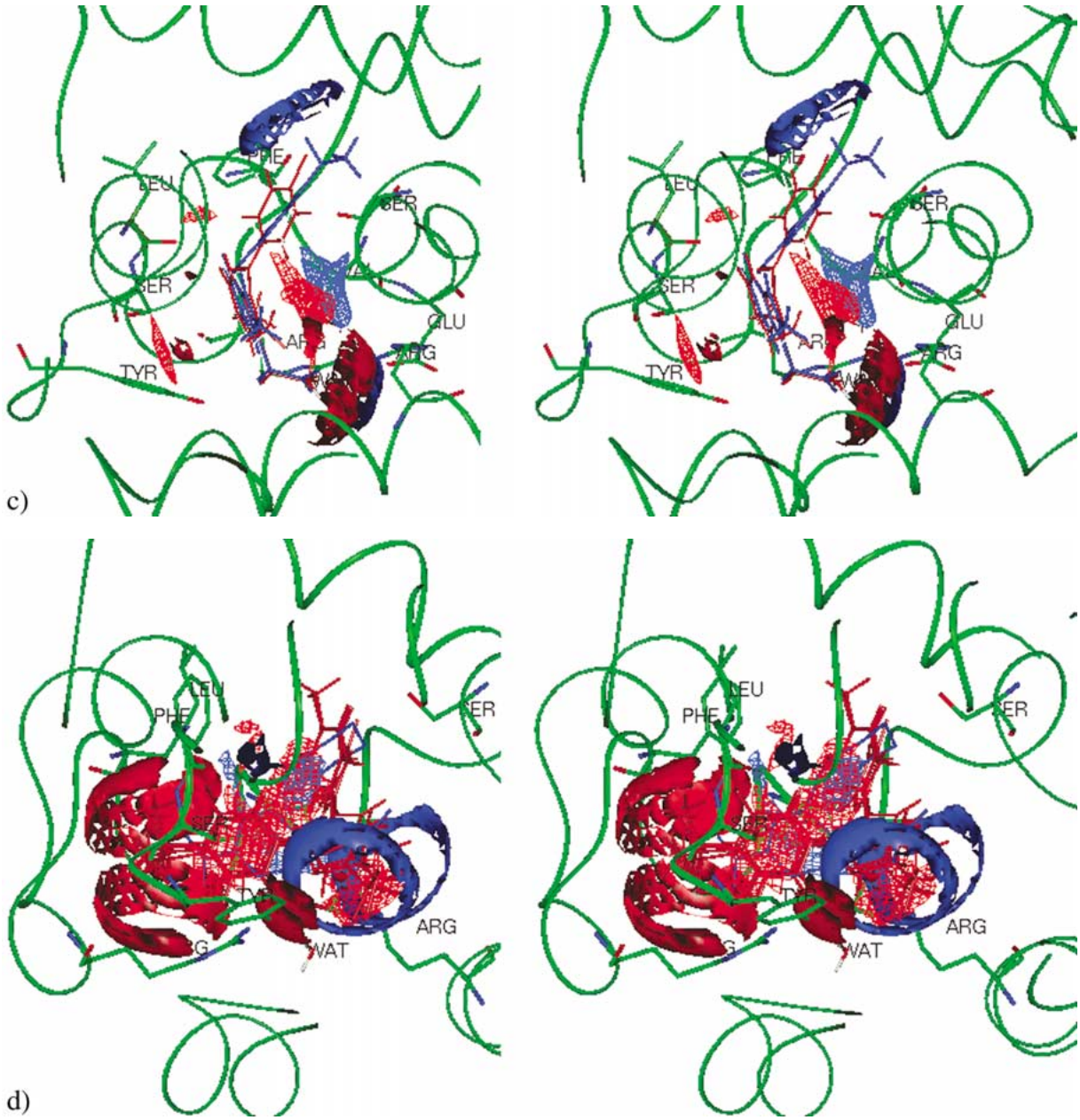

Figure 11. Continued.

the second or third ring tend to generate energetically favourable interactions in the fourth region (Phe^{518} and Tyr^{385}) for the less active compounds. The selective inhibitors interact closely with main-chain atoms of Leu^{352,} Ser^{353} and Val^{523} in the zones surrounding the first aromatic ring. The Val^{523} residue permits access to the side pocket of the main cyclooxygenase channel. The sulphonamide or sulfone moiety of selective COX-2 inhibitors inserts into this side pocket and forms a stable complex, which is responsible of selective inhibition [25]. The Val523 → Ile mutation renders the mutant protein resistant to time-dependent inhibition by diarylheterocycles [48–49].

GRID force field

Graphic representations of the contour plots of van der Waals (C3) and hydrogen-bonding (OH) probes

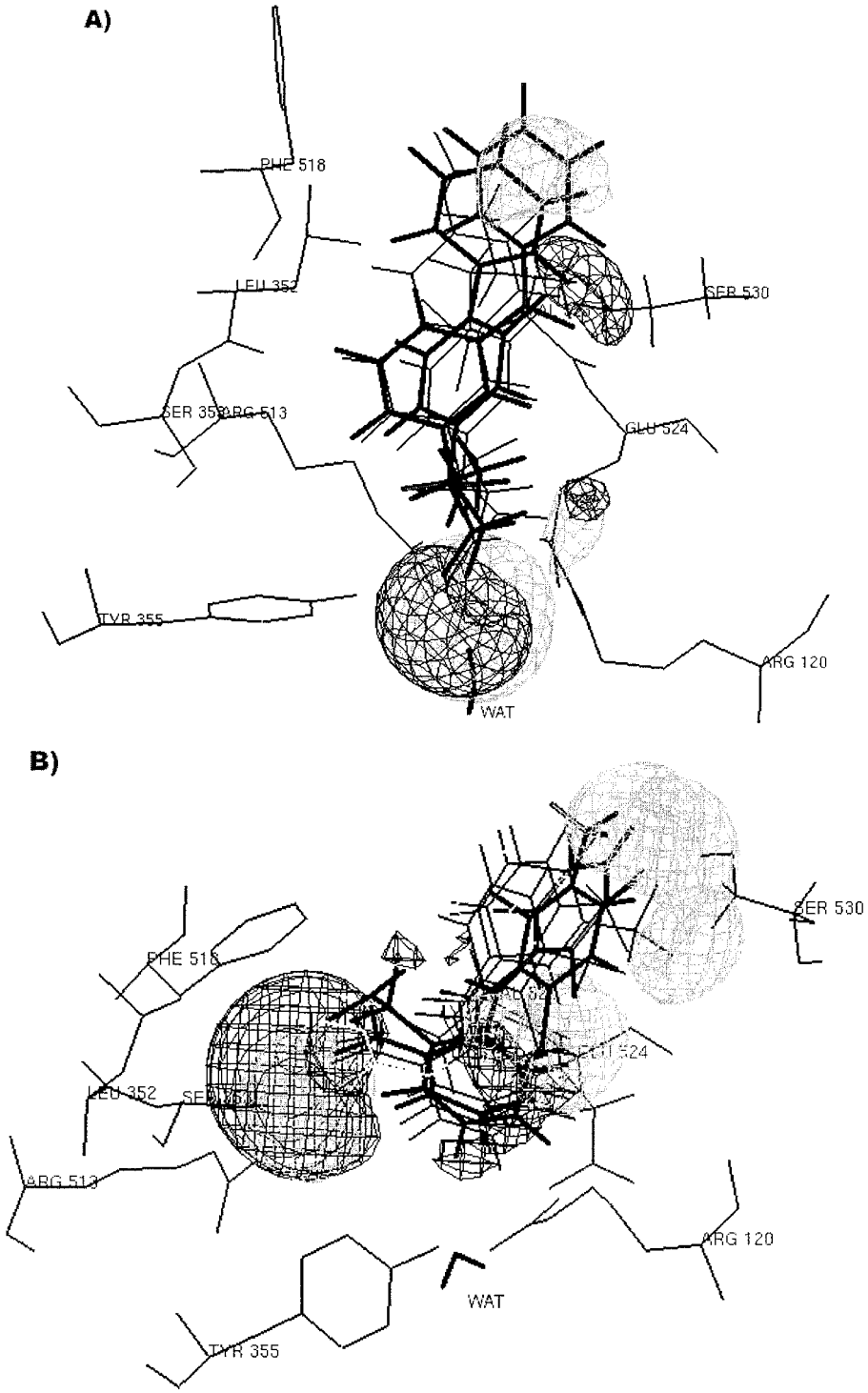

Figure 12. 3D MEP representations calculated at the HF/6-31G(d) level. The isopotential lines at −20 kcal/mol are shown in the cyclooxygenase-binding site (grey) of human PGHS-2. Only water and residues relevant to the discussion are displayed. a) Global superposition of S-flurbiprofen (black), S-ketoprofen (black), S-naproxen (grey) and S-ibuprofen (grey). b) Model of meclofenamate (black), diclofenac (black), mefenamate (grey), flufenamate (grey) and niflumate (grey). c) Model of *cis*-indomethacin and sulindac (black). d) Model of SC-558 (black), SC-58125 (black), SC-57666 (black), celecoxib (black) and NS-398 (grey).

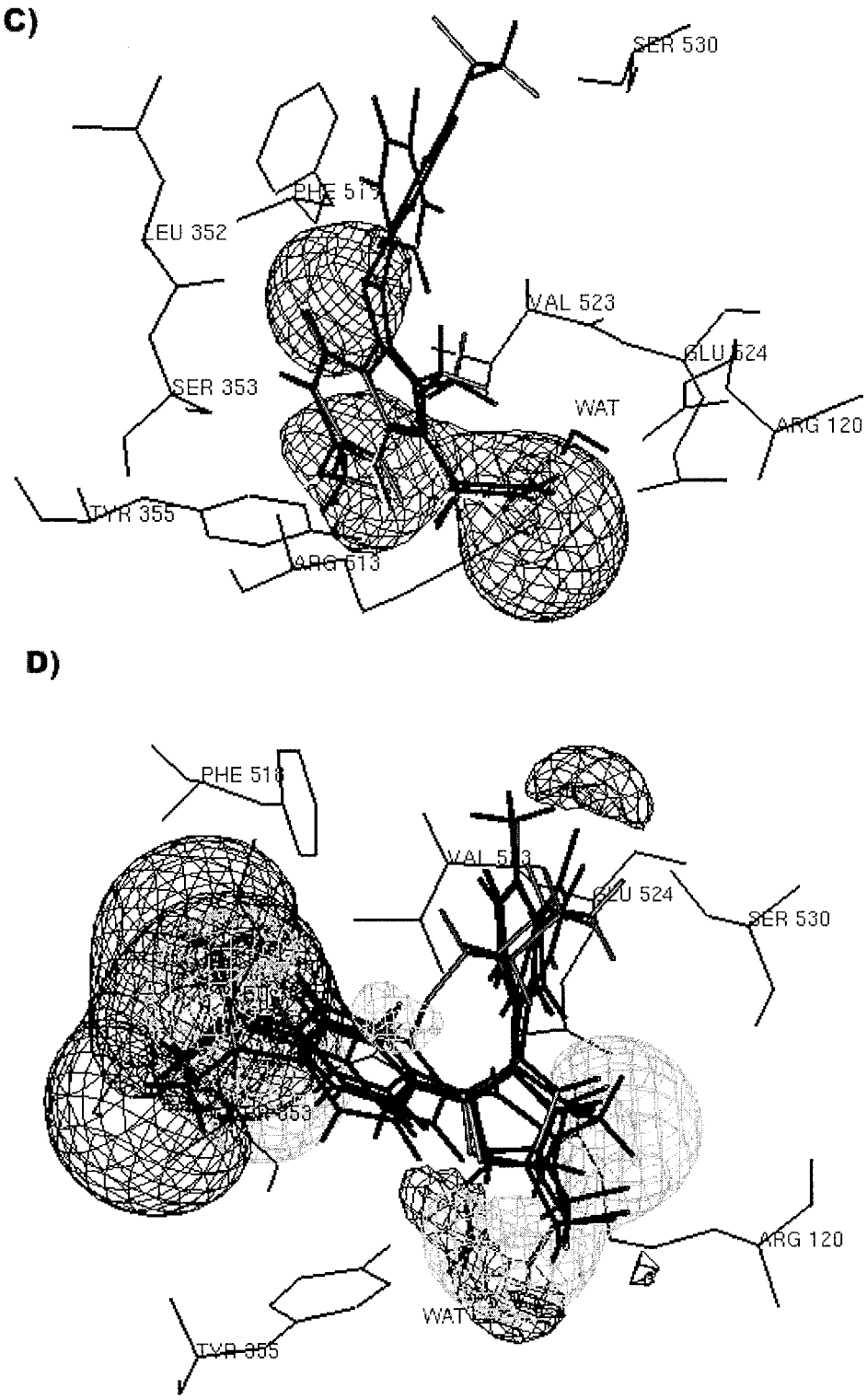

Figure 12. Continued.

are shown in Figure 11. They show regions where variations of steric or hydrophilic properties in the structural features of the compounds lead to increases or decreases in activity. The linear (solid) contour plot shows red-coloured regions where increased steric (hydrophilic) property is associated with enhanced activity.

The favourable steric region is close to the tensor between the two aromatic rings and the nonsulphonamide-containing phenyl ring, for the selective COX-2 inhibitors. The presence of a favourable hydrophilic zone close to the sulphonamide group points out the relevance of this region in the COX-2 side pocket binding. The entry gate to the second pocket of COX-2, which involves Val^{523}, is quite hydrophobic, due to the presence of the side chains of Val^{349}, Leu^{352}, Tyr^{355}, Val^{523}, Ala^{527} and Phe^{518}. Conversely, the inner part is relatively polar and inside this region the hydrogen–bond donor interacts favourably with the side chain of Gln^{192}, His^{90}, Arg^{513} and finally with the carbonyl oxygen of Phe^{518}. The interaction of charged groups inside this region should be particularly strong because of the presence of the negatively charged side chain Glu^{524} and the positively charged side chain of Arg^{120}.

It is important to recall that the COX-1 and COX-2 structures show a closed conformation where Arg^{120} maintains a salt-bridge with Glu^{524}. In COX-2 the closed conformation can be transformed into an open form owing to the competitive interaction with Arg^{513} that can modify the closed conformation between $Arg^{120}$and Glu^{524}. Non-selective COX-2 inhibitors like flurbiprofen generally have a carboxylate moiety, which can destroy the salt-bridge between Arg^{120} and Glu^{524} in both COX-1 and COX-2, which probably leads to the same conformational state at the bottom of the NSAID binding site for the two isoforms.

It is interesting to note that in our model for inhibitor-COX-2 complexes, a water molecule participates in the dynamic hydrogen-bonding network at the polar active site entrance together with residues Arg^{120}, Tyr^{355}, Glu^{524} and Arg^{513}. The hydrophilic favourable contour observed (Figure 11D) at the lower part of the heterocycle for the selective COX-2 inhibitors may be related to the ability of the compounds to bind such a water molecule.

Molecular electrostatic potential maps (MEP)

2S-Phenylpropionic acids

Figure 12A shows the topological features of 3D isopotential maps determined at the HF/6-31G(d) level (an isocontour value of −20 kcal/mol is used). The torsion between aromatic rings and the general topological features of the MEP contours allowed us to distinguish S-flurbiprofen and S-ketoprofen (linear contour plot shows black-coloured regions) from S-ibuprofen and S-naproxen (linear contour plot in grey regions). For S-flurbiprofen and S-ketoprofen the negative isopotential contours around F or O atoms are absent in the MEP maps of S-ibuprofen and S-naproxen. Only the extended negative region around the carboxylic group and on the first aromatic ring were retained, while the negative region of attractive potential to an approaching electrophile around the R1-substituent disappears (Table 3).

The global superimposition yields a good overlap of the common negative regions of the MEP localised around the carboxylic group. In contrast, the isopotential contours are very different in active time-dependent compounds (flurbiprofen and ketoprofen), characterised by a significant hook-shaped protrusion with vertex on the minimum of the carboxyl group, which extends around the entrance of the cyclooxygenase cavity between Arg^{120}, Tyr^{355}, Glu^{524} and Arg^{513}.

Fenamates and diclofenac acids

The isopotential contours (Figure 12B) show that the MEP negative region extends over the carboxyl and amino groups, and that an additional minimum is placed around the first or second aromatic ring. The isopotential regions for meclofenamate and diclofenac (linear contour plot in black-coloured regions) reveal an extended negative surface around N1 and the chlorine atoms, with two relative minima at the sides of the N1-H bond (Table 3). These are the only compounds that adopt an almost perpendicular arrangement between the aromatics rings (75° and 69°, respectively), because the chlorine atoms cause maximal twisting of the phenyl ring, and could show a better fit to the receptor. For mefenamate and flufenamate (linear contour plot in grey regions), the two phenyl rings are oriented at 50° and 44°, respectively. Furthermore, in flufenamate there is an isolated negative region in the terminal part of the 3D map, corresponding to the relative minimum on fluorine. Niflumate has an isolated negative region near the nitrogen atom in the first ring.

Table 3. Molecular electrostatic potential (MEP) minimum energy in kcal/mol and minimum location to a reference atom group computed from HF/6-31G(d) wavefunction.

Molecular electrostatic minimum (MEP) in kcal/mol						
Compound	COO-	R1-SO2	R1	R2	R3	NH/Nar bridge
S-Flurbiprofen	−70.6		−32.5			
S-Ketoprofen	−71.1		−70.2			
S-Naproxen	−73.2			−74.5		
S-Ibuprofen	−74.6			−17.7		
Diclofenac	−71.3		−13.8			−23,5
Meclofenamate	−73.2		−16.0			−36.2
Mefenamate	−73.7			−20.7		−22.8
Flufenamate	−70.0			−26.3		−31.4
Niflumate	−61.9			−29.7	−76.3	−43.7
Indomethacin	−74.1		(CO)	(OCH3)	(Cl)	
			−62.1	−78.8	−10.2	
Sulindac	−63.3			(F)	(SO)	
				−36.5	−97.3	
Celecoxib		−74.7		−25.1		−61.5
SC-58125		−80.5		−23.6		−54.7
SC-558		−80.4		−22.9		−52.6
SC-57666		−87.2			−32.4	(C9)
						2.5
NS-398		−69.2		(NO2)		(O)
				−57.6		−50.5

It also has an extended negative region in the terminal part of the 3D map corresponding to the fluorine. The molecular charge distributions of meclofenamate and diclofenac create a negative electrostatic potential around the bridging amino group, whereas those of the non-time-dependent inhibitor compounds in the same region become repulsive towards electrophile (Table 3).

Indomethacin and sulindac acids

In the corresponding 3D map for the indomethacin (Figure 12C) the negative isopotential is localised in an extended region around the indole ring and in the region above the oxygen atoms. The MEP topology is very similar in sulindac, meclofenamate and S-flurbiprofen. The isopotential contours present about the same shape, characterised by a significant hook-shaped protrusion which extends below the plane of the indol ring and ends just above it.

Diarylheterocyclics and NS-398

The MEP topologies for diarylheterocyclic compounds (Figure 12D) localise a similar extended region characterised by positive MEP values on the whole molecule and two or three negative zones in lateral regions. There is a negative surface (linear contour plot in black-coloured regions) surrounding a depth global minimum at the sulphonamide or methylsulfoxide groups and around the heterocyclic ring bridge between the phenyl rings. Structures of COX-2 cocrystalized with SC-558 indicate that the phenylsulfonamide moiety fits into the extra nook made accessible by Val^{523} [25]. The Arg^{513}, probably facilitates binding in this nook, which is within bonding distance of the sulphonamide group. Curiously, inhibition by the methylsulfoxide inhibitor NS-398 (grey-coloured regions) results from interaction with Arg^{120} and not Arg^{513}. NS-398 binds the COX-2 active site similarly to acidic NSAIDs and inhibits the $Arg^{120} \rightarrow$ Glu COX-2 mutant only competitively [47]. The MEP topology for the diarylheterocyclic and NS-398 compounds showed similar shapes characterised

by a significant hook-shaped protrusion with vertex on the minimum at the lower part of the heterocycle bridge between the phenyl rings, which extends around the entrance of the cyclooxygenase cavity between Arg^{120}, Tyr^{355}, Glu^{524} and Arg^{513}. The MEP topology for the selective COX-2 is very similar to that of meclofenamate, diclofenac and indolacetic (Table 3).

Discussion

Comparison of any PGHS-1 with any PGHS-2 enzyme leads to a sequence identity of 60%. Consistent with the high sequence identity, the overall structures of PGHS-1 and PGHS-2 are highly conserved (24). The COX active sites of PGHS-1 and PGHS-2 are very similar, the only differences in the residues of the binding site being Ile → Val ^{523} and His → Arg^{513} substitutions [16]. The PGHS-2 structure (Figure 3) possesses a second internal pocket extending off the NSAID binding site. In PGHS-2 the volume of the primary inhibitor binding site and the secondary pocket is calculated to be 394 $Å^3$, whereas the volume of the NSAID binding site of the PGHS-1 is 316 $Å^3$ [45].

The structural studies on murine PGHS-2 have shown that the conformation of the free enzyme in the crystal is very similar to those of the complexes with inhibitors. Therefore, the binding of inhibitors does not greatly perturb the resting structure. Surprisingly, the channel mouth is more restricted in the free enzyme, and the reported flexible nature of the human PGHS-2 binding site was taken into account in our molecular dynamics simulations, which were carried out for all the orientations of NSAIDs suggested by the automated docking program.

Implication of active site hydration on the selectivity

Kinetic analysis demonstrated that isoform selectivity was attained via elimination of the time-dependent component of inhibition on PGHS-1, but time-dependent inhibitors on PGHS-2 [23]. Owing to variations in assay design and sources of COX activity used throughout the literature, it is difficult to compare kinetic behaviour and inhibitory potency of the various NSAIDs with respect to the different PGHS isoforms.

The role of water molecules that participate in the dynamic hydrogen-bonding network at the polar active site entrance together with residues Arg^{120}, Tyr^{355}, Arg^{513} and Glu^{524} has been examined (Figures 8–9). The inhibitory activities for 16 inhibitory compounds have been rationalised in terms of the dynamic stability of such hydrated complexes. Particularly, it can be deduced that PGHS-2 produces a stable complex between the inhibitor, one water molecule and the amino acids Arg^{120} and Tyr^{355} only for the time-dependent arylpropionic (flurbiprofen and ketoprofen), fenamate (meclofenamate), indolacetic (indomethacin), diclofenac and selective COX-2 (SC58125, SC57666, SC558, NS398 and celecoxib) inhibitors. In contrast, stable complexes with the time-independent inhibitors (naproxen, ibuprofen and mefenamate) are also found, but they do not involve a water molecule, which moves away from its original position in the hydrogen-bonding network. These results are in agreement with the existence of a favourable hydrophilic region for all time-dependent inhibitors (Figure 11). These findings, in conduction with behaviour of the complexes together with the parallelism with the activities gives support to the COX-2 inhibitory mechanism by NSAIDs.

The role of the hydrogen-bond network in the mouth of the active site

The interaction energies of Arg^{120} and Arg^{513} with Glu^{524} residues in the cyclooxygenase cavity for all the inhibitor-COX-2 complexes were also examined. Electrostatic interactions of Arg^{120} of PGHS-2 with S-naproxen, S-ibuprofen and of Arg^{513} with mefenamate and flufenamate likely explain the fact that the disruption of the hydrogen-bond between Arg^{120}, Arg^{513} and Glu^{524} contributes to the competitive binding inhibition (Table 1). The balance between electrostatic interactions of Arg^{120} and Arg^{513} of PGHS-2 with selective-COX-2 and indolacetics may contribute to the fact that the hydrogen-bond network may predominate in the tightened form. Likewise, the balanced interactions of Arg^{120}/Arg^{513}/Tyr^{355} of PGHS-2 with meclofenamate and diclofenac can underlie the fact that the tightened form of the hydrogen bond between Arg^{120}, Arg^{513} and Glu^{524} contributes to the slow binding inhibition. The equilibrium between the two hydrogen-bonding arrangements forms a structural constriction and is an important determinant of NSAID binding, whereas in the tightened conformation the Arg^{120}/Glu^{524} hydrogen bonding network locks the substrate into a catalytically competent conformation.

The mouth of the active site of the NSAID-bound enzyme appears to be wider than that of the unbound enzyme, which may result, because arachidonate and

NSAIDs open the active site [52]. This enzyme conformation is likely stabilised by formation of the same network of hydrogen bonds between aminoacid side chains at the mouth of the cyclooxygenase active site that stabilises the binding of time-dependent inhibitors. Following oxygenation, a conformational rearrangement of arachidonate occurs that could disrupt the hydrogen-bonding network leading to release of PGG_2. Since time-dependent NSAIDs cannot undergo oxygenation, the nonproductive hydrogen bond-stabilised complex they form dissociates only slowly. Thus, time-dependent inhibition may be a serendipitous outcome of a catalytic mechanism evolved in PGHS to ensure fidelity of the cyclooxygenase reaction.

Comparative binding energy analysis

The activities calculated by the COMBINE model (Figure 10A) were in general quite similar to the experimental values, with the exception that the activity of flurbiprofen and ketoprofen were underestimated and that of ibuprofen, naproxen, mefenamate and flufenamate were overestimated. The most important residues in terms of steric and electrostatic interactions (Table 1) are located in four regions. One region is located in a hydrophobic cavity formed by Phe^{381}, Tyr^{385} and Ser^{530}. A second cavity involves Met^{113}, Val^{349}, Tyr^{355}, Ser^{353} and hydrophobic residues like Leu^{352}, Tyr^{355}, Phe^{518}, Val^{523}. The third region encompasses the binding site of sulphonamide or sulphonyl, which interact with His^{90}, Gln^{192} and Arg^{513}. Finally, the fourth region is at the mouth of the cyclooxygenase active site and mediates binding of time-dependent inhibitors with a water molecule and the residues Arg^{120} and Tyr^{355}.

The carboxylic acid moiety of all (2S)-phenylpropionic inhibitors forms a salt bridge with Arg^{120}, the two carboxylate oxygen atoms of the inhibitor lying between 1.40 and 1.60 Å from one of the guanidine nitrogens. The electrostatic interaction leads to a stable complex between inhibitor, one water molecule and the residues Arg^{120} and Tyr^{355}, which influences the overall inhibitory effect only for the time-dependent inhibitors (Figure 11). In addition, one carboxylic acid oxygen of indomethacin lies < 2.5 Å from the phenolic hydroxyl of Tyr^{355}. The side chains lining the channel below the inhibitor surround it and render it inaccessible to solvent. The efficiency of PGHS-2 inhibition by (2S)-phenylpropionics, sulindac and indomethacin increased when the magnitude of interaction with Arg^{120} increased.

Flurbiprofen is representative of the 2-phenylpropionic acid class of NSAIDs that are relatively non-specific for PGHS isozymes. It causes a time-dependent inhibition of the two PGHS, but fails to cause a time-dependent inhibition of $Arg^{120} \rightarrow Glu^{120}$ mutation of hPGHS-2 [47, 48]. Thus, as observed with oPGHS-1 [16], the Arg^{120} group of hPGHS-2 is necessary for both efficient binding and time-dependent inhibition of hPGHS-2 by 2-phenylpropionic acid class of NSAIDs.

SC-58125, SC-558, SC-57666 and celecoxib binds the COX active site with the sulphonyl or sulphonamide group, which interacts with His^{90}, Gln^{192} and Arg^{513}. One oxygen atom forms a hydrogen bond to His^{90}, and the other oxygen is hydrogen bonded to Arg^{513}. The amide nitrogen forms a hydrogen bond to the carbonyl oxygen of Phe^{518}. However, if these bonds are reinforced through the simultaneous presence of other interactions (hydrophobic, hydrogen bonding, van der Waals), the binding becomes much stronger and is able to last much longer.

The role of Tyr^{355} residue in the time-dependent inhibition

Diclofenac and meclofenamate retained some inhibitory effects (potency was decreased 5–6 fold) against the mutation of hPGHS-2 ($Arg^{120} \rightarrow Glu^{120}$), but there is 1000-fold decrease in potency for NS-398 [23]. In our model for NS-398 the sulphonamide group interacts with the side chain of Arg^{120} and Tyr^{355} in a manner similar to the carboxylic group of (2S)-phenylpropionics, while the nitro group interacts with Arg^{513}. The change in inhibitory potency of NS-398 on mutation of hPGHS-2 ($Arg^{120} \rightarrow Glu^{120}$) was due to a difference in the kinetics of inhibition (time-dependent $\rightarrow$ time-independent). The time-dependent inhibition by diclofenac and meclofenamate is similar for the mutant hPGHS-2 albeit at a higher concentration of inhibitor, suggesting that the contribution to the binding of an ionic interaction with Arg^{120} is minimal [48].

Acetylation of Ser^{530} or its mutation to Met does not greatly affect the binding and inhibitory properties of S-flurbiprofen, S-ketoprofen, indomethacin and NS-398, but diclofenac and meclofenamic acid have lost all potency for inhibition of the serine modified forms of PGHS-2 [19]. This is consistent with the hypothesis that the increased bulk of Met or acetyled Ser

results in a steric hindrance, which prevents their interaction with Tyr^{355} in the active site of cyclooxygenase [51].

Tyr^{355} is known to be involved in the differential molecular mechanism of time-dependent inhibition of PGHS-2 with fenamics, (2S)-phenylpropionics and PGHS-2-selective inhibitors. Moreover, indomethacin and meclofenamate were incapable of inhibiting the mutation of hPGHS-2 ($Tyr^{355} \rightarrow$ Phe) [22] suggesting a role for Tyr^{355} in the time-dependent inhibition by indomethacin, diclofenac, and meclofenamate.

The role of Val^{523} residue in the time-dependent inhibition

Comparison of the crystal structures of COX-2 complexed with SC-558 and COX-1 complexed with flurbiprofen suggests that the identity of Val^{523} affects access to a side pocket in which the sulphonamide or sulphonyl moiety binds. As further support for the role of this residue in selectivity, mutagenesis of COX-1 and COX-2 at this site indicates that the presence of Val instead of Ile is sufficient to confer selectivity for a similar ligand, SC-58125 [50]. The role of Val^{523} as a determinant in the differential interaction of PGHS-2 with selective and non-selective inhibitors is patent from experiments with the $Ile^{523} \rightarrow$ Val PGHS-1 mutant, which showed increased potency of NS-398 to PGHS-1. Thus, a single aminoacid change at position 523 in PGHS-2 confers a PGHS-1 inhibitory profile for these PGHS-2 selective inhibitors. The Val^{523} mutations in PGHS-2 produced diverse responses to the inhibitor [49]. The $Val^{523} \rightarrow$ Ala mutant was susceptible to time-dependent inhibition by SC-58125 and NS-398, whereas the single mutation $Val^{523} \rightarrow$ Ileu, Glu, or Lys of PGHS-2 increased the IC_{50} values to >100 μM, which looks like PGHS-1 for the selective PGHS-2 inhibitors. The differences between the behaviour of wild-type PGHS-2 and the Val^{523} mutant demonstrate that even subtle changes at position 523 influenced the susceptibility to time-dependent inhibition, the increases in bulk or charge (Val → Ile, Glu or Lys) reducing the tendency of time-dependent inhibition and a decrease in bulk (Val → Ala) having little effect.

The van der Waals interactions (Table 1) between the ligand and Val^{523} were increased for selective COX-2 inhibitors (5.4–4.0 kcal/mol), indomethacin (4.6 kcal/mol), and sulindac (4.2 kcal/mol) *versus* meclofenamate (3.1 kcal/mol) and diclofenac (2.9 kcal/mol), while van der Waals interactions between the ligand and Ser^{530} in the zones surrounding the terminal aromatic ring were increased for meclofenamate and diclofenac (2.0 kcal/mol). The C3 probe with the GRID program (Figure 11B) mapped a large favourable interaction area around Val^{523} and Phe^{518} for the time-dependent inhibitors.

Analysis of molecular interaction fields

To discern the feasibility of the different binding modes, the regression equations were developed to estimate free energies of binding for COX-2 inhibitors. Inspection of the separate (van der Waals, electrostatics) contributions to the binding free energy revealed a marked dependence of the inhibitory activity with the electrostatic term, which indicate that diclofenac and meclofenamate are more effective in inhibiting the enzyme than the other compounds. Looking at the adjustable parameters, the negative coefficient for the electrostatic term is not clearly physically reasonable, it likely being related to the hydrophobic effect. However, loss of hydrogen bonds in the binding pocket relative to the free hydrated state is energetically unfavourable, and an energy penalty of around 2 kcal/mol could be applied for each H-bond lost [40]. In contrast, the coefficient of the van der Waals component is positive, which means that a better van der Waals interaction leads to a good steric fit and enhance binding.

Only the van der Waals interaction energy term could explain the differences in binding affinities between selective and non-selective PGHS-2 inhibitors. The CoMFA studies by Marot et al. [53] suggested a good correlation between steric and electrostatic molecular fields and the activities registered for the selective COX-2 inhibitors. Overall, for this set of 16 inhibitors, a squared correlation coefficient $r^2 = 0.69$ was obtained and provides one measure of the quality of the fit (Figure 10B).

All the active time-dependent inhibitors show MEPs (Figure 12) with a negative-conical surface with their vertex on a water molecule that participate in the dynamic hydrogen-bonding network at the polar active site entrance together with residues Arg^{120}, Tyr^{355}, Arg^{513} and Glu^{524}. Thus, as observed with oPGHS-1 [16], the Arg^{120} group of hPGHS-2 is necessary for both efficient binding and time-dependent inhibition of hPGHS-2 by 2-phenylpropionic acid class of NSAIDs. This hypothesis is consistent with the proposal by On-Yee So and co-workers [21], and Luong et al. [46] that the equilibrium between two hydro-

gen bonding arrangements (Arg^{120}/Glu^{524}/Tyr^{355} and Arg^{513}/Glu^{524}/Tyr^{355}) is responsible for the allosteric activation and that disruption of this equilibrium contributes to the slow binding inhibition. They suggested the ability of the channel to move between open and closed conformations that allow both substrates and inhibitors to reach the internal binding site.

The central channel of the NSAID-binding pocket of PGHS-2 has been estimated to be about 17% larger than that of PGHS-1. This increased size may simply allow inhibitors to bind more tightly in the PGHS-2 active site, reducing the relative importance of ionic interactions with Arg^{120} or permitting more avid binding of nonacidic inhibitors in PGHS-2. Moreover, the substitution of Val^{523} in PGHS-2 for Ile^{523} in PGHS-1 permits access to a pocket or nook near the mouth and adjacent to the central channel of the binding pocket, increasing the volume of the PGHS-2 NSAID binding site about 25% compared to PGHS-1. This extra size is essential [54–55] for selective inhibition of PGHS-2 by diarylheterocycles (Figure 11D), and binding in this nook is probably also facilitated by Arg^{513}, which is within bonding distance of the sulphonamide group of these compounds.

These results are consistent with previous studies that indicated that diarylheterocycles associate rapidly and reversibly with COX-2 isoform and then undergo a slow transition leading to a more tightly bound complex. Lanzo et al. [26] suggested a structural three-step model to explain the kinetic differences in time-dependent versus time-independent binding of SC299 with the COX isoforms. In the first step SC299 binds the broad opening region that leads from the membrane-binding domain to the constriction that separates the upper part of the channel, which is the cyclooxygenase active site. In the second step the inhibitor moves past the constriction comprised of Arg^{120}/Glu^{524}/Tyr^{355} and Arg^{513}/Glu^{524}/Tyr^{355} to the cyclooxygenase active site. Finally, it inserts into the side pocket bordered by Val^{523}. Insertion of the sulphonamide or sulphone moiety into the side pocket accounts for the stability of the complex and results in an essentially irreversibly inhibited enzyme that is responsible for time-dependent inhibition. Not all time-dependent PGHS-2 inhibitors are reversible slow binding inhibitors; NS-398 is selective irreversible inhibitor of PGHS-2. This compound appears to form an enzyme-inhibitor complex, which promotes inactivation of the enzyme in the absence of substrate.

From the non-selective NSAIDs (ketoprofen) inhibitors selectivity may be reached by introducing the characteristic sulphonyl group [56]. Novel tetrahydro-2H-isoindoles without sulphonyl group have been prepared as selective COX-2 inhibitors. Structural modifications established that a bicycle ring appended to the pyrrole nucleus and 4,4difluoro substitution on the phenyl rings were optimal for high inhibitory potency [57]. These results suggest that the mechanism of interaction with the active site of COX-2 is different from that of the reference selective inhibitors, but the selectivity of these compounds was less potent than for celecoxib or rofecoxib.

In general the stability of the inhibitor-COX2 complex for the non-selective inhibitors is determined by the equilibrium between two hydrogen bonding arrangements (Arg^{120}/Glu^{524}/Tyr^{355} and Arg^{513}/Glu^{524}/Tyr^{355}) that is responsible for the allosteric activation and that disruption of this equilibrium contributes to the slow binding inhibition. However, for the selective COX-2 inhibitors the insertion of polar group into the side pocket accounts for the stability of an enzyme-inhibitor complex, which promotes inactivation of the enzyme in the absence of substrate.

Conclusions

This paper examines the time-dependent PGHS-2 inhibitors and their interactions with the receptor. From the X-ray crystallographic binding studies, it has been possible to use a structure-based ligand design strategy to determine which interactions make a significant contribution to the biological activity. We have established the importance of considering explicit water molecules that participate in the dynamic hydrogen-bonding network at the polar active site entrance together with residues Arg^{120}, Tyr^{355}, Arg^{513} and Glu^{524}. The inhibitory activities observed have been rationalised in terms of the dynamic stability of such hydrated complexes. Detailed knowledge of the role of the water molecules in the active site will be useful for further studies. When using an appropriate alignment of the compounds considered, both COMBINE and Linear Response methods (comparable correlation coefficient, $r^2 = 0.77$) offer results valuable to rationalise the differences in activity within the series. Furthermore, the combined use of the two approaches allows to validate the results and provides a more reliable interpretation of the results.

Inspection of the separate contributions to the binding free energy revealed a marked dependence of the

inhibitory activity with the electrostatic term. However, only the van der Waals interaction energy term could explain the differences in binding affinities between selective and non-selective PGHS-2 inhibitors. The increased volume of the PGHS-2 NSAID binding site (about 25%) compared to that in PGHS-1 is essential for selective inhibition of PGHS-2, and binding in this nook is probably also facilitated by Arg^{513} and Val^{523}.

The stability of the inhibitor-COX2 complex for the non-selective inhibitors is the equilibrium between two hydrogen bonding arrangements (Arg^{120}/Glu^{524}/Tyr^{355} and Arg^{513}/Glu^{524}/Tyr^{355}) that is responsible for the allosteric activation and that disruption of this equilibrium contributes to the slow binding inhibition.

However, all the selective COX-2 compounds have the lowest van der Waals interaction energies and the largest molecular volumes. For the selective inhibitors and fenamates the insertion of a polar group into the side pocket, which interacts with His^{90}, Gln^{192} and Arg^{513}, accounts for the stability of an enzyme-inhibitor complex, which promotes inactivation of the enzyme in the absence of substrate.

Acknowledgements

The authors thank Dr. A. Ortiz, Dr. J. Villà, Dr. M.M. Garrett Morris and Dr. Peter J. Goodford for provision of the software Combine, Mepsim, AutoDock v. 3.0, and GRID. We also thank Dr. J. Luque for helpful discussions and the CESCA for providing computational support in ab initio calculations.

References

1. Kulmacz, R.J. and Lands, W.E.M., In Prostaglandin and Related Substances: A Practical Approach (Benedetto, C., Mc Donald Gibson, R.G., Nigam, S. and Slater, T.F., eds) (1987), 209–227, IRL Press, Washington, D.C.
2. Smith, W.L., Marnett, L.J. and D.L. DeWitt, Prostaglandin and thromboxanes biosynthesis. In: Pharmac. Ther. Vol. 49 (1991) 153–179, Taylor, C.W. (ed). Pergamon Press. London.
3. Kulmacz, R.J., Palmer, G. and Ah-Lim Tsai., Mol. Pharm. 40 (1991) 833.
4. Ah-Lim Tsai, Kulmacz, R.J. and Palmer, G., J. Biol. Chem. 270 (1995) 10503.
5. Vane, J.R., Bakhle, Y.S. and Botting, R.M.. Annu. Rev. Pharmacol. Toxicol., 38 (1998) 97.
6. Lecomte, M., Laneuville, O., Chuan Ji, DeWitt, D.L. and Smith, W.L., J. Biol. Chem. 269 (1994) 13207.
7. Barnett, J., Chow, J., Ives, D., Chiou, M., Mackenzie, R., Osen, E., Nguyen, B., Tsing, S., Bach, C., Freire, J., Chan, H., Sigal, E. and Ramesha, C., Biochim. Biophys. Acta., 1209 (1994) 130.
8. Earnest, D.L., Hixson, L.J. and Alberts, D.S., J. Cell. Biochem. Suppl. 161 (1992) 156.
9. Kargman, S.L., O'Neill, G.P., Vickers, P.J., Evans, J.F., Mancini, J.A. and Jothy, S., Cancer Res. 55 (1995) 2556.
10. DeWitt, D.L., Mol. Pharm., 55 (1999) 625.
11. Gierse, J.K., Koboldt, C., Walker, M.C., Seibert, K and Isakson, P.C., Biochem. J., 339 (1999) 607.
12. Scherrer, A., Fenamic Acids. In: Anti-Inflammatory and Anti-Rheumatic Drugs. Vol. 2 (1985). 65–85, K.D. Rainsford and M.R.C. Path (eds.) CRC Press, Inc. Florida, USA.
13. Lozano, J.J., López, M., Ruiz, J., Vazquez, I.J. and Pouplana, R., QSAR in the nonsteroidal antiinflammatory agents: The fenamic acids. In Trends in QSAR and Molecular Modelling'92. (1993), 560–562. C.G. Wermuth (ed). ESCOM, Leiden.
14. Ouellet, M. and Percival, D., Biochem. J., 306 (1995) 247.
15. Bhattacharyya, D.K., Lecomte, M., Rieke, C.J., Garavito, M.R. and Smith, W.L., J. Biol. Chem., 271 (1996) 2179.
16. Picot, D., Loll, P.J. and Garavito, R.M., Nature, 367 (1994) 243.
17. Loll, P.J., Picot, D. and Garavito, R.M., Nature Struc. Bio., 2 (1995) 637.
18. Loll, P.J., Picot, D., Ekabo, O. and Garavito, R.M., Biochemistry, 35 (1996) 7330.
19. Pouplana, R., Pérez, C., Sánchez, J., Lozano, J.J. and Puig-Parellada, P., J. Comput.-Aided Mol. Design., 13 (1999) 297.
20. Lozano, J.J., Pouplana, R. and Ruiz, J., J. Mol. Struc., (Theochem), 397 (1997) 59.
21. So, O., Scarafia, L.E., Mak, A.Y., Callan, O.H. and Swinney, D.C., J. Biol. Chem., 273 (1998) 5801.
22. Selinsky, B.S., Gupta, K., Sharley, C.T. and Loll, P.J., Biochem. 40 (2001) 5172.
23. Palomer, A., Pérez, J.J., Navea, S., Lorens, O., Pascual, J., García, L. and Mauleón D., J. Med. Chem., 43 (2000) 2280.
24. Mancini, J.A., Vickers, P.J., O'Neill, G.P., Boily, C., Falgueyret, J., and Riendeau, D., Mol. Pharm., 51 (1997) 52.
25. Kurumbail, R.G., Stevens, A.M., Gierse, J.K., McDonald, J.J., Stegeman, R.A., Pak, J.Y., Gildehaus, D., Miyashiro, J.M., Penning, T.D., Seibert, K., Isakson, P.C. and Stallings, W.C., Nature, 384 (1996) 644.
26. Lanzo, C.A., Sutin, J., Rowlinson, S., Talley, J. and Marnett, L.J., Biochem., 39 (2000) 6228.
27. Pouplana, R., Lozano, J.J. and Ruiz, J., J. Mol. Graph. Mod., 20 (2002) 329.
28. Biosym/MSI. Accelrys 9685 Scranton Road San Diego, USA.
29. Lozano, J.J., Pouplana, R., López, M. and Ruiz, J., J. Mol. Struc. (Theochem), 335 (1995) 215.
30. Moser P., Sallmann A. and Wiesenberg I., J. Med. Chem., 33 (1990), 2358.
31. Dhanaraj, V. and Vijayan, M., Acta Cryst., B44 (1988) 406.
32. Ruiz, J., López, M., Milà, J., Lozoya, E., Lozano, J.J. and Pouplana, R., J. Comput.- Aided Mol. Design, 7 (1993) 183.
33. Frisch, M.J., Head-Gordon, M., Trucks, G.W., Foresman, J.B., Schlegel H.B., Gill, P.M., Johnson, B.J., Robb, M.A., Cheesemann, J.R., Keith, T.A., Petersson, G.A., Montgomery, J.A., Raghavachari K., Al-Laham, M.A., Zakrzewski, V.G., Ortiz, J.V., Cioslowski, J., Stefanov, B.B., Nanayakkara, A., Challacombe, M., Binkley, J.S., Peng, C.Y., Ayala, P.Y., Chen, W., Wong, M.W., Andres, J.L., Gonzalez C., Replogle, E.S., Gomperts, R., Defrees, D.J., Fox, D.J., Baker J., Martin, R.L., Stewart, J.P. and Pople, J.A., Gaussian 94, Revision A.1. Gaussian Inc., Pittsburgh, PA, 1995.

34. Case, D.A., Pearlman, D.A., Caldwell, J.C., Cheatham, T.E., Ross, W.S., Simmerling, C., Darden, T., Merz, K.M., Stanton, R.V., Cheng, A., Vincent, J.J., Crowley, M., Fergusson, D.M., Radmer, R., Seibel, G.L., Singh, U.C., Weiner, P., Kollman P.A., AMBER5; University of California, San Francisco, (1997).
35. AutoDock: Automated Docking of Flexible Ligands to Receptors. Version 3.0 (1998). Morris, G.M., Goodsell, D.S., Halliday, R.S., Huey, R., Hart, W.E., Belew, R.K. and Olson, A.J. The Scripps Research Institute. La Jolla. CA.
36. Morris, G.M., Goodsell, D.S., Halliday, R.S., Huey, R., Hart, W.E., Belew, R.K. and Olson, A.J., J. Comp. Chem., 19 (1998) 1639.
37. Goodford, P.J, J. Med. Chem., (1985) 849.
38. GRIN, GRID, GRAB and GROUP version 16.0. Molecular Discovery Ltd., (1998).
39. Pastor, M., Cruciani, G. and Watson, K.A. , J. Med. Chem., 40 (1997) 4089.
40. Smith, R.H., Jorgensen, W.L., Tirado-Rives, J., Lamb, M.L., Janssen, P.A., Michejda, C.J., Kroeger Smith M.B., J. Med. Chem., 41 (1998) 5272.
41. Hansson, T., Marelius, J., Aqvist, J., J. Comput.-Aided Mol. Design., 12 (1998) 27.
42. Ortiz, A.R., Pisabarro M.T., Gago, F. and Wade, R.C., J. Med. Chem., 36 (1995) 2681.
43. Ortiz, A.R., Pastor, M., Palomer, A., Cruciani, G.,Gago, F. and Wade, R.C., J. Med. Chem., 40 (1997) 1136.
44. Sanz, F., Manaut, F., Rodriguez, J., Lozoya, E. and López de Briñas, E., J. Comput.-Aided. Mol. Des., 7 (1993) 337.
45. Luong, C., Miller, A., Barnett, J., Chow, J., Ramesha, C. and Browner, M.F., Nat. Struct. Biol., 3 (1996) 11927.
46. Rieke, C.J., Mulichak, A. M., Garavito, R.M. and Smith, W.L., J. Biol. Chem., 274 (1999) 17109.
47. Greig, G.M., Francis, D.A., Falgueyret, J.P., Ouellet, M.M., Percival, M.D., Roy, P., Bayly, C., Mancini, J.A. and O'Neill G.P., Mol. Pharm., 52 (1997) 829.
48. Gierse, J.K., Hauser, S.D., Creeley, D. P., Koboldt, C., Rangwala, S. H., Isakson, P.C. and Seibert, K., Biochem. J., 305 (1995) 479.
49. Guo, Q., Wang, L., Ruan, K. and Kulmacz, J., J. Biol. Chem., 271 (1996) 19134.
50. Wong, E., Bayly, C., Waterman, H.L., Riendeau, D. and Mancini, J.A., J. Biol. Chem., 272 (1997) 9280.
51. Cromlish, W.A. and Kennedy, B.P., Biochem. Pharmacol., 52 (1996) 1777.
52. Smith T., McCracken J., Kyun Shin, Yeon. and DeWitt D., J. Biol. Chem., 275 (2000) 40407.
53. Marot, C., Chavatte, P. and Lesieur, D., Quant. Struct. Act. Relat., 19 (2000) 127.
54. Gierse, J.K., McDonald, J.J., Hauser, Koboldt, C., Rangwala, S.H., and Seibert, K., J. Biol. Chem., 271 (1996) 15810.
55. Bambai, B. and Kulmacz, R.J., J. Biol. Chem., 275 (2000) 27608.
56. Palomer, A., Pascual, J., Cabré, M., Borrás, L., González, G., Aparici, M., Carabaza, M., Cabré, F., Garcia, M.L. and Mauleón, D., Bioorg. Med. Chem. Lett., 12 (2002) 533.
57. Portevin, B., Tordjman, Pastoureau, Ph., Bonnet, J. and Nanteuil, G., J. Med. Chem., 43 (2000) 4582.
58. Höskuldsson, A., PLS regression methods, J. Chemometrics, 2 (1988) 211.
59. Melissa, L., Plount Price and Jorgensen, W.L., J. Am. Chem. Soc., 122 (2000) 9455.
60. Filipponi, E., Cecchetti, V., Tabarrini, O., Bonelli, D. and Fravolini, A., J. Comput.-Aided Mol. Des., 14 (2000) 277.